1

AIR FORCE INSTITUTE OF TECHNOLOGY

AIR UNIVERSITY
UNITED STATES AIR FORCE

HIGH TEMPERATURE OXIDATION OF SILICON CARBIDE

THESIS

GAW/MC/72-11

Warren J. Miller
1 Lt USAF

SCHOOL OF ENGINEERING

Reproduced by
NATIONAL TECHNICAL
INFORMATION SERVICE
U S Department of Commerce
Springfield VA 22151

WRIGHT–PATTERSON AIR FORCE BASE, OHIO

DOCUMENT CONTROL DATA - R & D

(Security classification of title, body of abstract and indexing annotation must be entered when the overall report is classified)

1. ORIGINATING ACTIVITY (Corporate author) Air Force Institute of Technology (AFIT-EN) Wright-Patterson AFB, Ohio 45433	2a. REPORT SECURITY CLASSIFICATION Unclassified 2b. GROUP

3. REPORT TITLE

HIGH TEMPERATURE OXIDATION OF SILICON CARBIDE

4. DESCRIPTIVE NOTES (Type of report and inclusive dates)
AFIT Thesis

5. AUTHOR(S) (First name, middle initial, last name)

Warren J. Miller
1/Lt USAF

6. REPORT DATE June 1972	7a. TOTAL NO. OF PAGES 55	7b. NO. OF REFS 28
8a. CONTRACT OR GRANT NO. b. PROJECT NO. c. d.	9a. ORIGINATOR'S REPORT NUMBER(S) 9b. OTHER REPORT NO(S) (Any other numbers that may be assigned this report)	

10. DISTRIBUTION STATEMENT

Approved for public release; distribution unlimited.

Approved for public release; IAW AFR 190-17 **Keith A. Williams, 1st Lt., USAF** **Acting Director of Information**	12. SPONSORING MILITARY ACTIVITY

13. ABSTRACT

Thermogravimetric measurements were made for the oxidation of hot pressed silicon carbide at an oxygen pressure of 150 torr and at temperatures from 1300°C to 1600°C. Oxidized samples were then analyzed using X-ray, metallograph, and electron probe techniques.

The oxidation rate was found to increase with temperature. A sharp increase in the oxidation rate found between 1400°C and 1500°C was attributed to the pres of water vapor.

The products of oxidation were a carbon oxide and a protective layer of sil The silica was primarily amorphous with some tridymite or α-cristobalite.

DD FORM 1 NOV 65 1473

14. KEY WORDS	LINK A		LINK B		LINK C	
	ROLE	WT	ROLE	WT	ROLE	WT
High Temperature Oxidation						
Oxidation						
Silicon Carbide						
Carbide						
Silicon						
Silicon Dioxide						

HIGH TEMPERATURE OXIDATION OF SILICON CARBIDE

THESIS

Presented to the Faculty of the School of Engineering
of the Air Force Institute of Technology
Air University
in Partial Fulfillment of the
Requirements for the Degree of
Master of Science

by

Warren J. Miller, B.S.M.E.
1 Lt USAF

Graduate Air Weapons
June 1972

Approved for public release; distribution unlimited

10

Preface

This study was originally undertaken to investigate one part of a much larger problem shared by both the Air Force and the civilian technical community. The problem is to find suitable materials for high temperature environments. Since silicon carbide showed good mechanical properties at high temperatures, it was decided that its oxidation properties should be investigated.

The research was performed at Aerospace Research Laboratories (ARL), Wright-Patterson Air Force Base, Ohio. I am indebted to Dr. Henry Graham and Captain Hubert Davis for their assistance, valuable guidance and timely comments. I would also like to thank the many personnel of the Metallurgy and Ceramics Research Laboratory (ARZ) of ARL for their assistance in solving the many technical problems encountered. Special thanks also go to my thesis advisor, Captain Wes Crow, for his suggestions and guidance.

I especially want to thank my wife Carole for her gentle prodding and patient understanding, and my cat for keeping my feet warm during many long, cold nights.

Warren J. Miller

Contents

List of Figures

List of Tables

Abstract

Thermogravimetric measurements were made for the oxidation of hot pressed silicon carbide at an oxygen pressure of 150 torr and at temperatures from 1300°C to 1600°C. Oxidized samples were then analyzed using X-ray, metallograph, and electron probe techniques.

The oxidation rate was found to increase with temperature. A sharp increase in the oxidation rate found between 1400°C and 1500°C was attributed to the presence of water vapor.

The products of oxidation were a carbon oxide and a protective layer of silica. The silica was primarily amorphous with some tridymite or α-cristobalite.

HIGH TEMPERATURE OXIDATION
OF SILICON CARBIDE

I. Introduction

In recent years the application of ceramics for use in high-temperature environments has been extensively investigated. New advances in manufacturing techniques have prompted much of this interest. One particularly promising material is hot pressed silicon carbide. Its high melting point, high thermal conductivity, low coefficient of thermal expansion, and good high temperature strength properties make it attractive for uses at high temperatures. However, little is known about the oxidation behavior of this material at high temperatures.

The purpose of this study was, therefore, twofold. First, to determine a practical upper temperature limit for hot pressed silicon carbide, and second, to determine the reason for this limit. The basis for these determinations was thermogravimetric measurements of the oxidation behavior of the silicon carbide.

II. Literature Survey

The oxidation kinetics of silicon carbide have been extensively investigated in recent years. In most cases the investigations were conducted using silicon carbide powders. However, the oxidation kinetics observed with powders should also apply to the hot pressed silicon carbide investigated in this paper. Therefore, the literature survey that follows was conducted to gain needed insight into the oxidation of silicon carbide. A literature survey of silicon carbide oxidation, however, would not be complete without a literature survey of silicon oxidation. Both silicon and silicon carbide have similar oxidation kinetics and similar oxidation products. Therefore, a survey of silicon oxidation is also given.

Oxidation of Silicon

Investigations of silicon oxidation have been conducted in temperatures ranging from 500°C to 1400°C and in total pressures from 1 micron to 760 torr. Various oxidizing atmospheres have been used including wet and dry oxygen and carbon dioxide. In this section an attempt was made to summarize and compare the results of these investigations.

Brodsky and Cubicciotti (Ref 1) studied the oxidation of silicon over the temperature range from 950°C to 1160°C at an oxygen pressure of 20 torr. They found by measuring the decrease of pressure of oxygen in a closed system that the rate of oxygen consumption followed a parabolic law at 950°C and 1160°C. A logarithmic rate law was found to fit the data at the temperatures between 950°C and 1160°C. The oxide was reported to be "glass-looking" indicating an amorphous oxide, but X-ray patterns indicated a crystalline phase was also present. The authors believed the crystalline phase to be either α-cristobalite or quartz.

Law (Ref 2) studied the oxidation from 727°C to 1027°C in oxygen pressures from 10^{-3} torr to 5×10^{-2} torr. He found under all conditions that the oxidation rate followed a parabolic rate law where the rate constant increased with pressure. Law concluded that the rate-determining step was the diffusion of some reactant species through the oxide film and that the pressure dependence was due to the variation of the surface electrical field with pressure.

Evans and Chatterji(Ref 3) used a thermobalance to find oxidation rates from 1200°C to 1400°C in pure dry oxygen at one atmosphere. Their data fits a parabolic law except at short times (1 to 2 hours). The deviation at short times indicated a faster rate and was attributed to atomic surface roughness. The oxide layer was reported to be transparent cristobalite in all cases.

In addition to the above authors, McAdam and Geil (Ref 4), and Ligenzer and Spitzer (Ref 5) have also reported a parabolic rate law fit to their data. McAdam and Geil investigated temperatures from 500°C to 1000°C and Ligenzen and Spitzer studied the oxidation from 700°C to 1100°C. Because their information indicated the rate was parabolic and controlled by the diffusion of some species through the silicon dioxide layer, Jorgensen (Ref 6) ran modified-marker experiments to determine the diffusing species. Jorgensen found that oxygen was the diffusing species. To determine the form of the diffusing species, Jorgensen placed an electric field across an oxidizing sample. He found the oxidation enhanced with the field aligned such that the silicon was positive with respect to the gas and found the oxidation retarded when the field was reversed. It was his conclusion that the diffusing oxygen was primarily ionic.

Deal and Grove (Ref 7) have reported some discrepencies in the manner in which silicon oxidation data has been evaluated. In an attempt to correlate data from other authors with their own, Deal and Grove have theoretically derived a general relationship for the oxidation of silicon taking into account the reactions occurring at the two boundaries of the oxide layer and the diffusion process. The relationship is

$$X_o^2 + AX_o = B(t + \tau) \qquad (1)$$

where X_o is the thickness of the oxide layer, t is the time, and A, B, and τ are physico-chemical constants of the oxidation reaction. Solving the quadratic results in

$$\frac{X_o}{A/2} = \left[1 + \frac{t + \tau}{A^2/4B}\right]^{1/2} - 1 \qquad (2)$$

which gives the oxide thickness as a function of time. For large times Eq (2) reduces to the parabolic rate law, and for short times it reduces to a linear rate law. Deal and Grove were able to fit their data to Eq (2) as well as the data from other authors. Working with wet and dry oxygen at 760 torr from 700°C to 1200°C, they found that the oxidation rate increased with wet oxygen. By replacing the wet oxygen with wet argon the constants A and B in Eq (2) were not changed. From this, Deal and Grove inferred that the water was the oxidizing species.

Burkhardt and Gregor (Ref 8) looked at the oxidation of single-crystal silicon using ultra-dry oxygen. A temperature range of 900°C to 1200°C and a pressure range of 20 to 760 torr were studied. Two types of measurements were made. The first involved measuring the oxide thickness and the second involved measuring the change of volume of oxygen with time in a closed system at lower temperatures. The data for oxide thicknesses up to 5000Å fit a linear parabolic equation which would be in agreement with Deal and Grove. However, at high temperatures a simple parabolic rate was reported.

The above authors have been primarily concerned with the oxidation of silicon whenever a silicon dioxide layer develops. However, silicon may also oxidize to silicon monoxide which happens to be a gaseous phase. This would indicate that under proper conditions a protective layer of SiO_2 would not be formed. Instead, SiO would form which would not remain at the surface. Wagner (Ref 9) has discussed theoretically the conditions for the formation of SiO as well as SiO_2. He considered a silicon sample initially free of oxygen or oxide during heating in an O_2-He stream whose oxygen content was gradually increased. Wagner proposed that if the partial pressure P_{SiO} at the surface is less than the equilibrium partial pressure $P_{SiO(eq)}$ for the reaction

$$\frac{1}{2}\,Si(\ell) + \frac{1}{2}\,SiO_2(s) = SiO(g) \qquad (3)$$

then the silicon surface will remain bare. However, at higher oxygen concentrations P_{SiO} will reach $P_{SiO(eq)}$ and a protective SiO_2 layer may be formed. Therefore, Wagner proposed that an "active" to "passive" transition should occur if

$$P_{SiO} = P_{SiO(eq)} \qquad (4)$$

Wagner further derived equations to determine the oxygen partial pressure above which the silicon would no longer remain bare and the oxygen partial pressure below which an oxide would begin to volatilize. The values quoted in the report for 1410°C are $P_{O_2}(max) = 6.1\times10^{-3}$ atmospheres and $P_{O_2}(min) = 3\times10^{-8}$ atmospheres. This indicates a range of oxygen partial pressures where neither oxidation of the silicon nor volatilization of the oxide takes place.

Gulbransen and Jonsson (Ref 10) have investigated the active-passive transition for silicon. Their results are shown in Fig. 1. Wagner's equation and a similar equation derived by the authors are shown on the figure. These lines represent the theoretical values for the active to passive transition. The circles are actual data points.

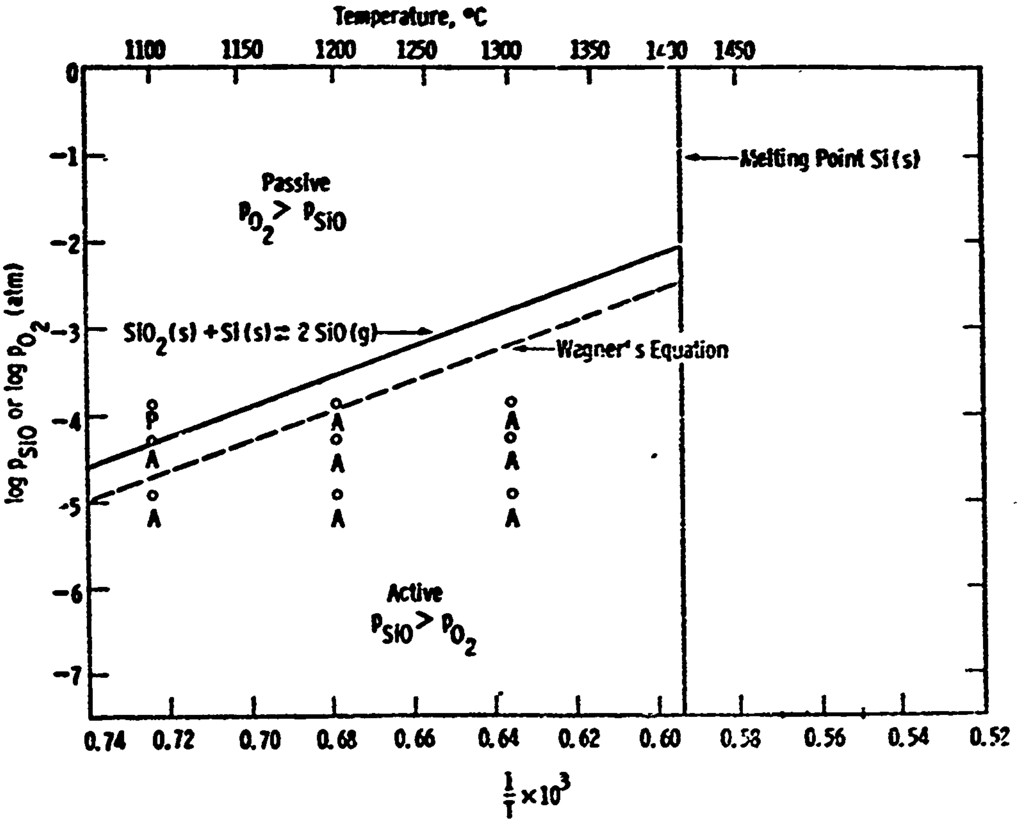

Fig. 1. Thermochemical Correlation for Active and Passive Oxidation of Silicon (Ref 10)

Under passive oxidation, the oxide layer which formed has been primarily amorphous, but as indicated, some crystalline phases of silica have been reported. The reason the crystalline phases formed may be due to one of two reasons. First, Brown and Kestler (Ref 11) have reported that glasses with added Al_2O_3 were found to devitrify to cristobalite more rapidly than ultra-pure silica glasses, implying that impurities may nucleate crystalline phases. Second, Wagstaff (Ref 12) found that water vapor enhanced crystallization.

From the above information it can be concluded that the oxidation of silicon may be either active or passive. If the oxygen partial pressure is great enough the oxidation in dry oxygen will be passive following the equation

$$Si + O_2 \longrightarrow SiO_2 \qquad (5)$$

and if the oxygen partial pressure is low enough the reaction will be active following the equation

$$2Si + O_2 \longrightarrow 2SiO \qquad (6)$$

From the data of Gulbransen and Jonsson the active to passive transition region will be governed by the equation

$$SiO_2(s) + Si(s) \rightleftarrows 2SiO(g) \qquad (7)$$

If passive oxidation occurs then the oxidation rate can be represented by a linear-relationship at short times and a parabolic relationship at long times. In wet oxygen the oxidation rate is observed to be higher than in dry oxygen because water becomes an oxidizing species. Finally it can be concluded that the oxide layer produced during passive oxidation is primarily amorphous silica with some cristobalite possible.

Oxidation of Silicon Carbide

The oxidation of silicon carbide although similar to silicon is more complex because of the addition of carbon. With silicon there were two equations which described the oxidation depending on the partial pressure of oxygen, but with silicon carbide there are many more than two equations. Table I from Humphrey et al. (Ref 13) enumerates several reactions between silicon carbide and oxygen. The data given by the authors also show that

TABLE I

Silicon Carbide-Oxygen Reactions

Reaction	ΔG° (Cal) 25°C	ΔG° (Cal) 1627°C
$SiC(s) + 2O_2(g) \rightleftarrows SiO_2(s) + CO_2(g)$	-279.2	-215.4
$SiC(s) + \frac{3}{2}O_2(g) \rightleftarrows SiO_2(s) + CO(g)$	-217.7	-187.2
$SiC(s) + O_2(g) \rightleftarrows SiO_2(s) + C(g)$	-184.9	-120.7
$SiC(s) + \frac{3}{2}O_2(g) \rightleftarrows SiO(g) + CO_2(g)$	-110.1	-144.5
$SiC(s) + O_2(g) \rightleftarrows SiO(g) + CO(g)$	- 48.6	-116.3
$SiC(s) + \frac{1}{2}O_2(g) \rightleftarrows SiO(g) + C(g)$	- 15.8	- 49.8
$SiC(s) + O_2(g) \rightleftarrows Si(s,\ell) + CO_2(g)$	- 81.9	- 86.5
$SiC(s) + \frac{1}{2}O_2(g) \rightleftarrows Si(s,\ell) + CO(g)$	- 20.4	- 58.3

these reactions are thermodynamically possible.

From the table it can be seen that the oxidation of silicon carbide may lead to silicon dioxide or silicon monoxide. This indicates that the work by Wagner cited earlier for silicon oxidation also applies to silicon carbide oxidation. Gulbransen and Jonsson (Ref 10) have investigated the active to passive transition for silicon carbide. Figure 2, similar to Fig. 1, shows three theoretical equilibrium equations and several actual data points. It can be seen from the figure that line C best represents the data. The equation for this line is equation C. From the figure it can also be seen that the transition from the active to the passive state

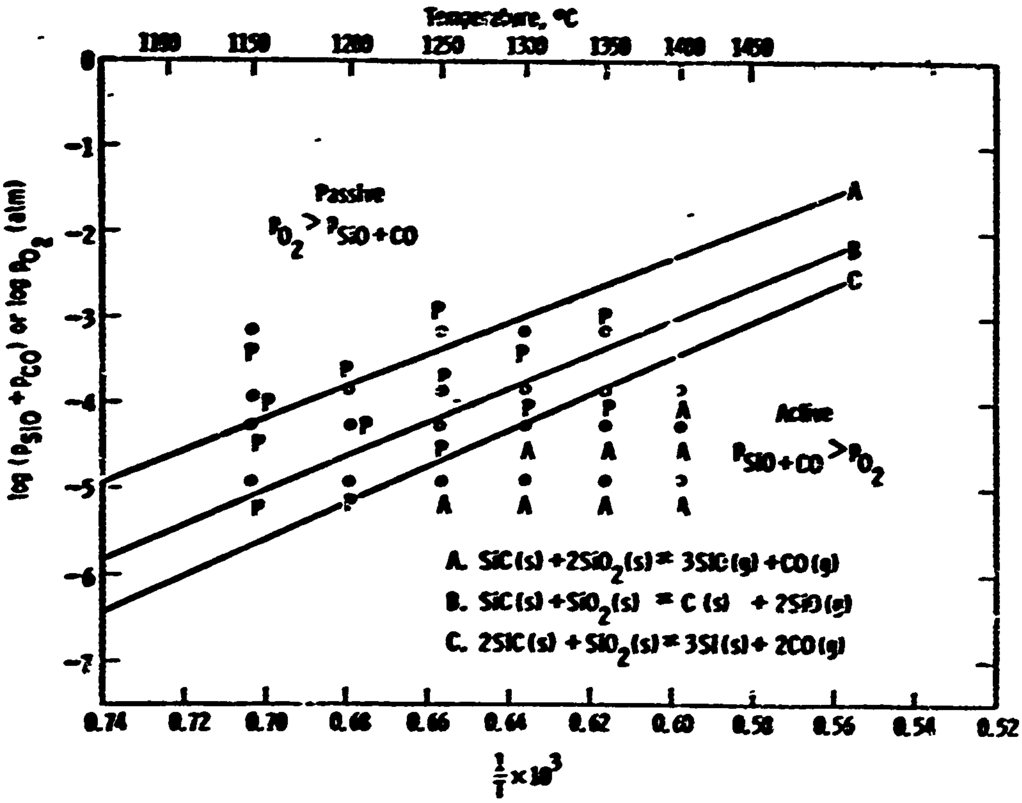

Fig. 2. Thermochemical Correlation for Active and Passive Oxidation of Silicon Carbide (Ref 10)

is expected to occur if at the surface of the sample the partial pressure P_{SiO+CO} is equal to the equilibrium partial pressure $P_{SiO+CO(eq)}$.

Keys (Ref 14) has also studied the active oxidation of silicon carbide. He found the reaction to follow the equation

$$SiC(s) + O_2(g) \rightleftarrows SiO(g) + CO(g) \qquad (8)$$

Using dried oxygen and sintered silicon carbide, he found the active oxidation to obey a linear rate law showing a marked temperature dependence. Because of the marked temperature dependence, the author believed that the rate controlling step was the reaction itself and not the diffusion of oxygen to the surface.

Gulbransen et al. (Ref 15) have also investigated the active oxidation of silicon carbide. Using single crystals of silicon carbide the authors found that the kinetics of active oxidation depended on the pressure or the gas flow. The products of active oxidation were determined to be carbon monoxide and silicon monoxide.

Although there have been some investigations of the active region, most investigators have confined their studies to the passive region of oxidation. Suzuki (Ref 16) studied the oxidation of powdered silicon carbide in dry oxygen at one atmosphere for 50 hours at temperatures from 819°C to 1400°C. He found that the oxide formed was cristobalite above 1350°C and amorphous below 1200°C. He also found that between 1300°C and 1400°C the oxidation reaction generally followed a parabolic rate.

Adamsky (Ref 17) also studied the oxidation of silicon carbide powder. However, where the measurements of Suzuki were weight gain of the powder, the measurements of Adamsky were weight gain of a carbon dioxide collecting ascarite bulb. His results are shown in Fig. 3. Each data point represents an average of several determinations. Oxygen at one atmosphere was purified to remove H_2, H_2O, CO_2 and CO. The oxide formed was amorphous over the entire temperature range. Rates were determined to follow a parabolic law over the entire range. The large

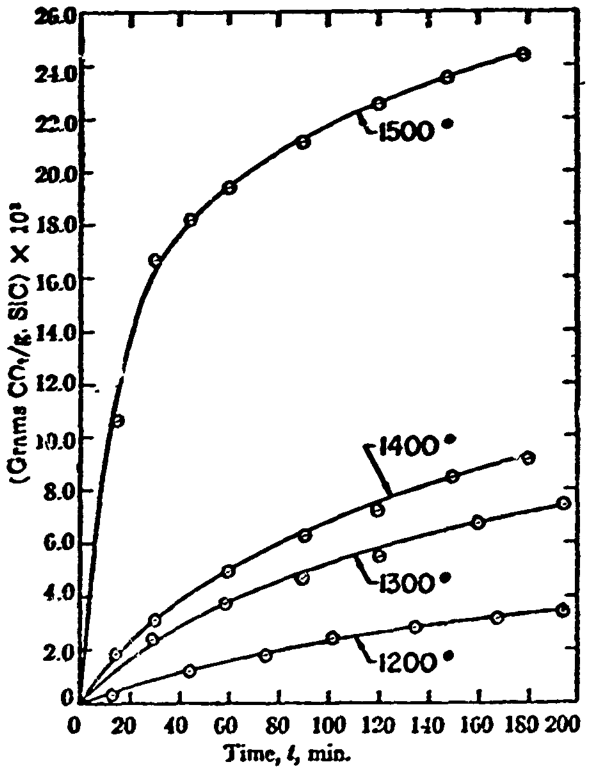

Fig. 3. Measured Weight Gain of CO_2 Per Gram of SiC versus Time (Ref 17)

jump between 1400°C and 1500°C was attributed to a very rapid surface reaction between silicon carbide and oxygen that controlled the reaction until a sufficient layer of SiO_2 formed to produce a diffusion-controlled mechanism.

Jorgensen et al. (Refs 18, 19, and 20) in a series of papers, studied the oxidation of silicon carbide powders and the effects of oxygen pressure and water vapor on the oxidation rates. Temperatures ranged from 900°C to 1600°C. For dry, flowing oxygen at one atmosphere the authors' results are shown in Fig. 4 where R is the fraction of completion of oxidation of a carbide particle. The straight lines in the figure indicate that a parabolic rate law was followed. The reaction product, SiO_2, was amorphous at temperatures below 1200°C. Above 1200°C the amorphous film transformed to cristobalite after an incubation period. The transformation was found to correspond to the change in slope of the curves in Fig. 4. The nucleation rate of the cristobalite was found to be very small in the dry oxygen, but water vapor in the gas greatly accelerated the nucleation rate in agreement with Wagstaff (Ref 12). The authors found that with changing oxygen partial pressure, the diffuse rate constant K shown in the equation (derived from Fig. 4)

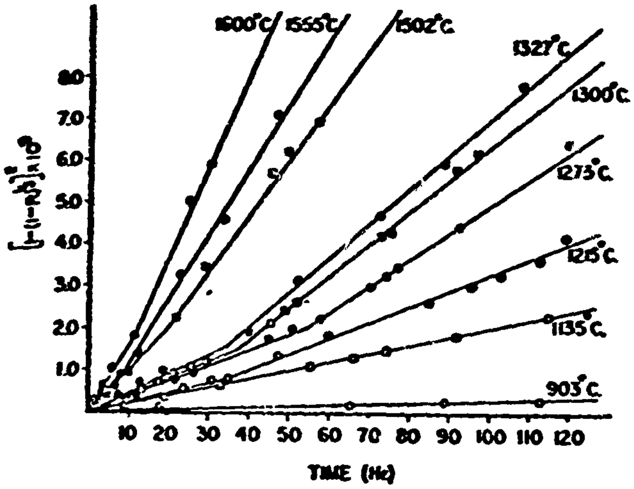

Fig. 4. Plot of the Parabolic Equation Corrected for a Change in Area vs Time for -325+400 Mesh SiC (Ref 18)

$$\left[1 - (1 - R)^{1/3}\right]^2 = Kt \qquad (9)$$

was found to vary with the logarithm of the oxygen partial pressure according to the theory of oxidation of thin films as proposed by Engell and Hauffe (Ref 21). This theory involves the transport of cations through the film to the surface. The theory follows the parabolic rate law where the parabolic constant can be defined as

$$K = A \ln P_{O_2} + B \qquad (10)$$

where A and B are constants. Based on this theory the authors believe the rate is controlled by the diffusion of an ionic species in agreement with previous investigations of silicon oxidation seen earlier. To determine the effect of water vapor different partial pressures of water vapor were used in a flowing oxygen stream at one atmosphere. Compared with dry oxygen, wet oxygen gave increased rates of oxidation. The authors believed that in both cases the diffusing species were the same and the increase was due to a change in the nature of the oxide film. With the wet oxygen atmosphere the oxide film was found to be cristobalite at 1218°C and tridymite at higher temperatures.

Antill and Warburton (Ref 22) have studied the behavior of silicon, a self-bonded silicon carbide, and pure silicon carbide in carbon dioxide, water vapor, oxygen, carbon monoxide, vacua, and helium at 1000°C to 1300°C. When silica films formed, a parabolic rate was obeyed for times up to 500 hours and there was little difference between the three materials. The activities of the oxidants were found to decrease in the order, water vapor, oxygen, and carbon dioxide, with carbon monoxide being inert. For oxidation in water vapor and carbon dioxide, the silica films were predominantly composed of α-cristobalite. The authors deduced that in the case of dry oxygen the diffusing species were oxygen ions, but in the case of water vapor the diffusing species were hydroxyl ions. The authors also deduced that under active oxidation, silica was an intermediary and the rate determining step was the desorption of the gaseous products.

The latter deduction is partially based on the studies of Pultz and Hertl (Refs 23 and 24) who found that above temperatures of 1250°C silica and silicon carbide react to give silicon monoxide and carbon dioxide. By a process of elimination the authors deduced that the rate controlling step was either desorption or transport from the reaction area of the reaction products. Adding gases to the reaction had the effect of depressing the reaction. For inert gases, the reaction rate was depressed with an increase in pressure or molecular weight.

Key (Ref 14) in his work with self-bonded silicon carbide found that in the passive region for all temperatures and pressures investigated the oxide layer contained bubbles, many of which had reached the surface and ruptured. He assumed that a reaction like the one shown to occur by Hertl and Pultz could nucleate a gas bubble on some defect or discontinuity at the carbide surface. He then thermodynamically proved that with the diffusion of oxygen to the defect the bubble could grow according to the equation

$$SiC(s) + \frac{3}{2} O_2(g) \rightleftarrows CO(g) + SiO_2(s) \qquad (11)$$

and then eventually rupture.

From the above discussions on the oxidation of both silicon carbide and silicon the following general conclusions can be made:

1. In the active region, silicon carbide oxidizes according to the equation

$$SiC(s) + SiO_2(s) \longrightarrow 2SiO(g) + CO(g) \qquad (12)$$

where the SiO_2 is an intermediate phase.

2. In the passive region the silicon carbide oxidizes according to the equation

$$SiC + \frac{3}{2} O_2 \rightarrow SiO_2 + CO \qquad (13)$$

3. The silica layers formed under passive oxidation are composed of amorphous SiO_2, α-cristobalite, or tridymite depending on the temperature and the oxidizing atmosphere.

4. Under passive oxidation the silica layers are likely to bubble and rupture.

5. At high temperatures (> 1500°C) a reaction between the silica layer and the silicon carbide can be expected. Therefore, at lower temperatures, vaporization of SiO can be expected to be small. Although not mentioned earlier this is in agreement with Abraytis and Mayauskas (Ref 25).

III. Experimental Apparatus and Materials

In this chapter only the apparatus and materials directly related to the thermogravimetric measurements will be discussed. The remaining equipment used in this study will be described as necessary in the chapter on experimental procedures.

Sample Materials

The silicon carbide samples used for this study were generously donated by Norton Company. The samples were 1/8 inch square bars of research grade silicon carbide cut from larger hot pressed billets. Density of the bars was within 5% of the theoretical density of 3.22 grams per cubic centimeter. The bars were originally bending specimens, and bars from different billets varied in composition. This compositional difference did not affect the results except in one case: the bars containing appreciable amounts of tungsten and cobalt behaved quite differently from those containing only small amounts of these constituents. Table II is a mass spectrographic analysis (by Battelle Memorial Institute, Columbus, Ohio) of a typical sample for each of these cases.

Furnace

Figure 5 is a cutaway view of the furnace and adjoining hardware showing only necessary details for the discussion that follows. Further details may be obtained in Ref 26.

The furnace was essentially a sealed stainless steel pipe with a recrystalized alumina tube (1-3/4" ID, 2" OD × 17") separating the sample area from the tungsten heating element. A high vacuum was held on the heating element side of the tube to prevent exposure of the element to

TABLE II

Mass Spectrographic Analysis of Silicon Carbide (ppma)

Element	SiC I	SiC II	Element	SiC I	SiC II	Element	SiC I	SiC II	Element	SiC I	SiC II
Li	1.	1.	Ni	70.	40.	In	< 0.6	< 0.1	Yb	< 0.1	< 0.1
Be	< 0.3	< 3. *	Cu	50.	30.	Sn	300.	6.	Lu	< 0.03	< 0.03
B	100.	100.	Zn	1.	4.	Sb	6.	0.6	Hf	0.3	< 0.1
F	30.	50.	Ga	< 5.	<10. †	Te	< 3. *	< 0.1	Ta	< 3.	10.
Na	50.	30.	Ge	1.	< 1.	I	0.03	< 0.03	W	150.	6000.
Mg	100.	100.	As	0.3	0.5	Cs	< 0.05	< 0.05	Re	< 0.05	< 0.5
Al	High	High	Se	< 1. *	< 1.	Ba	1.	2.	Os	< 0.1	< 0.1
P	20.	20.	Br	< 0.4	< 0.4	La	1.	0.5	Ir	< 0.05	< 0.05
S	50.	70.	Rb	1.	0.3	Ce	1.	0.5	Pt	< 0.3	< 1.
Cl	20.	200.	Sr	0.5	0.5	Pr	0.3	0.1	Au	< 0.3	< 0.1
K	5.	5.	Y	1.	1.	Nd	2.	0.4	Hg	< 0.1	< 0.2
Ca	15.	15.	Zr	20.	20.	Sm	0.2	< 0.1	Tl	< 0.05	< 0.05
Sc	< 1.	< 2.	Nb	1.	<30. §	Eu	< 0.06	< 0.06	Pb	400.	< 1.
Ti	100.	200.	Mo	1.	20.	Gd	0.1	< 0.1	Bi	5.	< 0.1
V	200.	300.	Ru	< 0.1	< 0.1	Tb	< 0.03	< 0.03	Th	< 0.03	< 0.03
Cr	500.	30.	Rh	10.	< 0.2	Dy	0.2	< 0.1	U	< 0.3	< 0.03
Mn	30.	20.	Pd	< 0.1	< 0.1	Ho	0.05	< 0.03			
Fe	1000.	500.	Ag	0.1	< 0.06	Er	0.1	< 0.1			
Co	50.	3000.	Cd	< 0.3	< 0.3	Tm	< 0.03	< 0.03			

*Memory from previous sample †Matrix interference §Tungsten interference

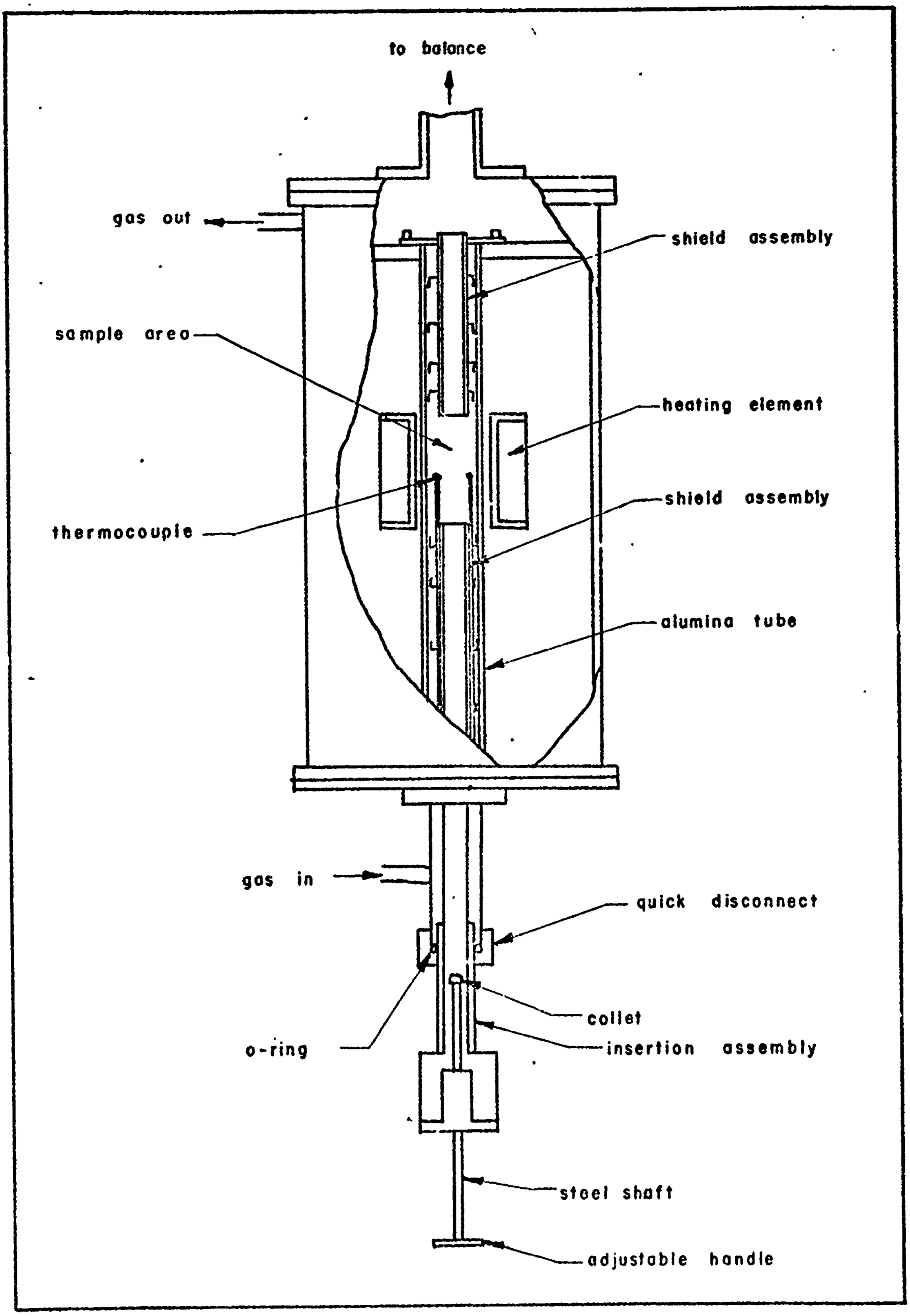

Fig. 5. Cutaway of Oxidation Furnace and Insertion Assembly

oxidizing atmospheres. The high vacuum was monitored by using a thermocouple gauge and an ionization gauge.

Temperature control was either manual or automatic. In the manual mode a constant amount of power was supplied to the heating element. However, constant power did not maintain a constant temperature in the sample area. To maintain constant temperature the power to the heating element was varied using the automatic mode.

The automatic mode functioned by amplifying the output of one of two thermocouples (Pt - 6 Rh, Pt - 30 Rh) in the sample area, comparing it with a bucking voltage provided by a digital set point circuit, and then as necessary switching in or out of the heating element circuit an adjustable, low-resistance rheostat. The output of the second thermocouple was directed to a potentiometer for monitoring the sample area temperature. With this arrangement of the two thermocouples, the temperature in the sample area was maintained within ±2°C.

Besides the basic equipment described above, some additional features were incorporated in the furnace. These features included two shield assemblies, one at each end of the furnace tube extending to within two inches of the center of the sample area; and an insertion assembly for inserting samples from the bottom of the furnace.

The two shield assemblies were constructed and added to the furnace to prevent excessive heat flow from the sample area and thus allow the furnace to be opened at temperature without risk of thermal shock cracking the furnace tube. The assemblies also helped maintain a constant temperature in the sample area. The shield tubes (7/8" ID, 1-1/8" OD × 6-1/2") were made of high temperature mullite, and the shields (1-3/4" diameter) were made of alumina disks. Platinum wire was used to attach the shields to the tubes. In the lower shield assembly, grooves were cut in the tube and shields so that two 1/8" two-hole alumina rods could be incorporated to hold the two thermocouples.

Caps for the thermocouple rods were also machined from alumina to cover the thermocouples and thus cut down on vaporization of the platinum from the thermocouples.

The insertion assembly was machined from brass and aluminum to be used in conjunction with a commercially available O-ring sealed, bearing for a 3/8 inch diameter stainless steel shaft. The upper end of the steel shaft was drilled and colleted to accept and hold securely a two hole 3/16 inch by 9 inch alumina rod. The upper portion of this rod is shown later in this paper in Fig. 9. To the lower end of the steel shaft was attached an adjustable handle so that the travel of the shaft could be limited. With the insertion assembly, a sample could be introduced into the center of the sample area without disturbing the environment in the sample area. The lower portion of the insertion assembly was machined so that it could be quickly disconnected from the upper portion. This allowed rapid retrieval of anything which may have inadvertently fallen into the furnace, as well as providing access to the sample holding alumina rod. Caution was taken to be sure that the furnace tube was never open at both ends at the same time. With both endsopen, a chimney effect could be created, possibly cracking the tube and/or destroying delicate electronic equipment in the balance.

Gas System

Figure 6 shows a schematic drawing of the gas handling system used in this study. Research grade oxygen containing impurities of water vapor, carbon dioxide, carbon monoxide, hydrogen, argon, and nitrogen was used

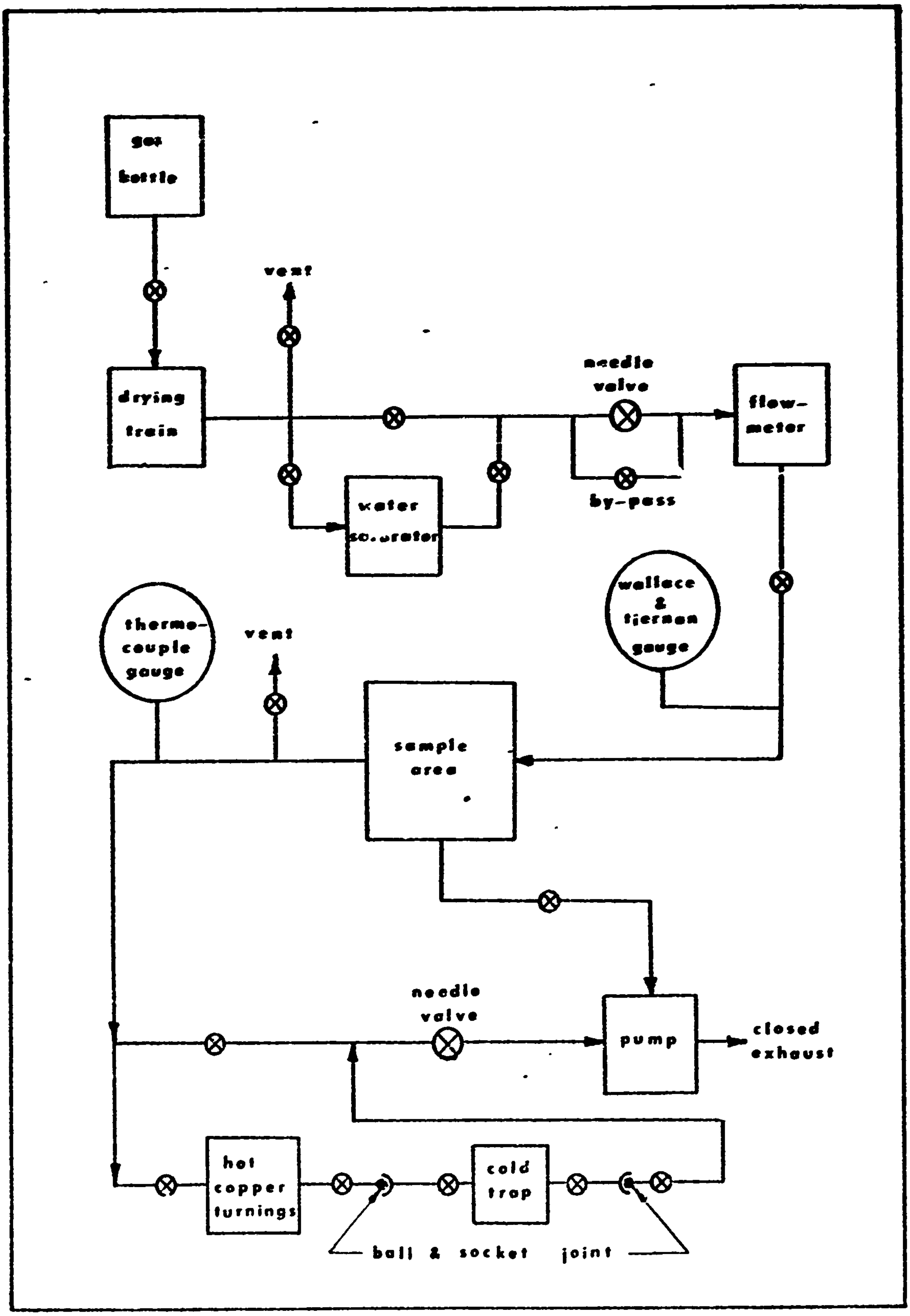

Fig. 6. Schematic of the Gas System

as the gas source. To remove the water vapor, carbon dioxide, carbon monoxide, and hydrogen, the gas was subjected to a drying train containing, in order, the following: magnesium perchlorate, indicator drierite, ascarite, copper pellets at 100°C, copper oxide at 100°C, ascarite, indicator drierite, and magnesium perchlorate.

After leaving the drying train, the gas, if desired, was subjected to a water saturator which consisted of bubbling the treated oxygen through distilled water. The gas then flowed through a variable-area flowmeter (Matheson T-600) and into the sample area. The gas could then leave the sample area by one of three paths: either (1) directly to a two cubic feet per minute mechanical pump; (2) through a needle valve and then to the pump; or (3) through a carbon dioxide trap, the needle valve, and then the pump. Upon leaving the pump the gas entered a closed exhaust system to prevent accumulation of toxic or explosive gases.

The carbon dioxide trap was made of two components as shown in Fig. 6. The first component was a glass tube containing copper-copper oxide turnings at 300°C to convert carbon monoxide to carbon dioxide, and the second component was a liquid nitrogen cold trap designed to freeze out the carbon dioxide. The cold trap was made of glass and appropriately valved so that it could be removed from the system to recover the solid carbon dioxide. The carbon dioxide was recovered by allowing the cold trap to warm up to ambient temperature and flowing the evolved gases through a weighed ascarite bulb. The difference in before and after weights was the amount of carbon dioxide recovered. Figure 7 shows the system for recovery of the carbon dioxide. A second ascarite bulb was used in series with the weighed bulb so that contamination by the ambient atmosphere was minimized.

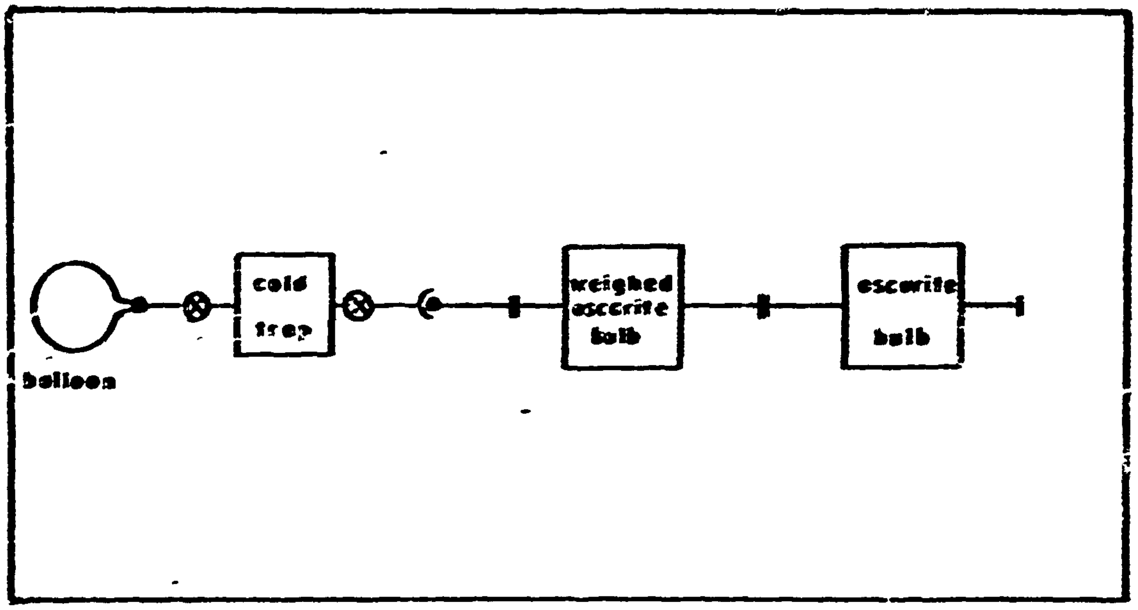

Fig. 7. Carbon Dioxide Collection System

When flowing gas was desired, the two needle valves in the system were adjusted to maintain the desired flow and pressure. This pressure was measured one of two ways. For the range 1 atmosphere to 0.001 atmosphere a Wallace-Tiernan gauge was used and for the range 1000 microns to 1 micron a thermocouple gauge was used.

Balance Arrangement and Sample Suspension

Figure 8 shows a simplified view of the balance and sample suspension system. The balance was a Cahn RH Electrobalance (see Ref 27 for the principle of operation) with its output directed to a two speed (15 minutes per inch and 5 minutes per inch) Leeds and Northrup Speedomax H, AZAR recorder.

The output of the balance was adjustable by means of a gain control so that the weight gain across the full scale of the recorder could be selected from various predetermined values. The output was also biased using a manually adjusted potentiometer so that weight change measurements

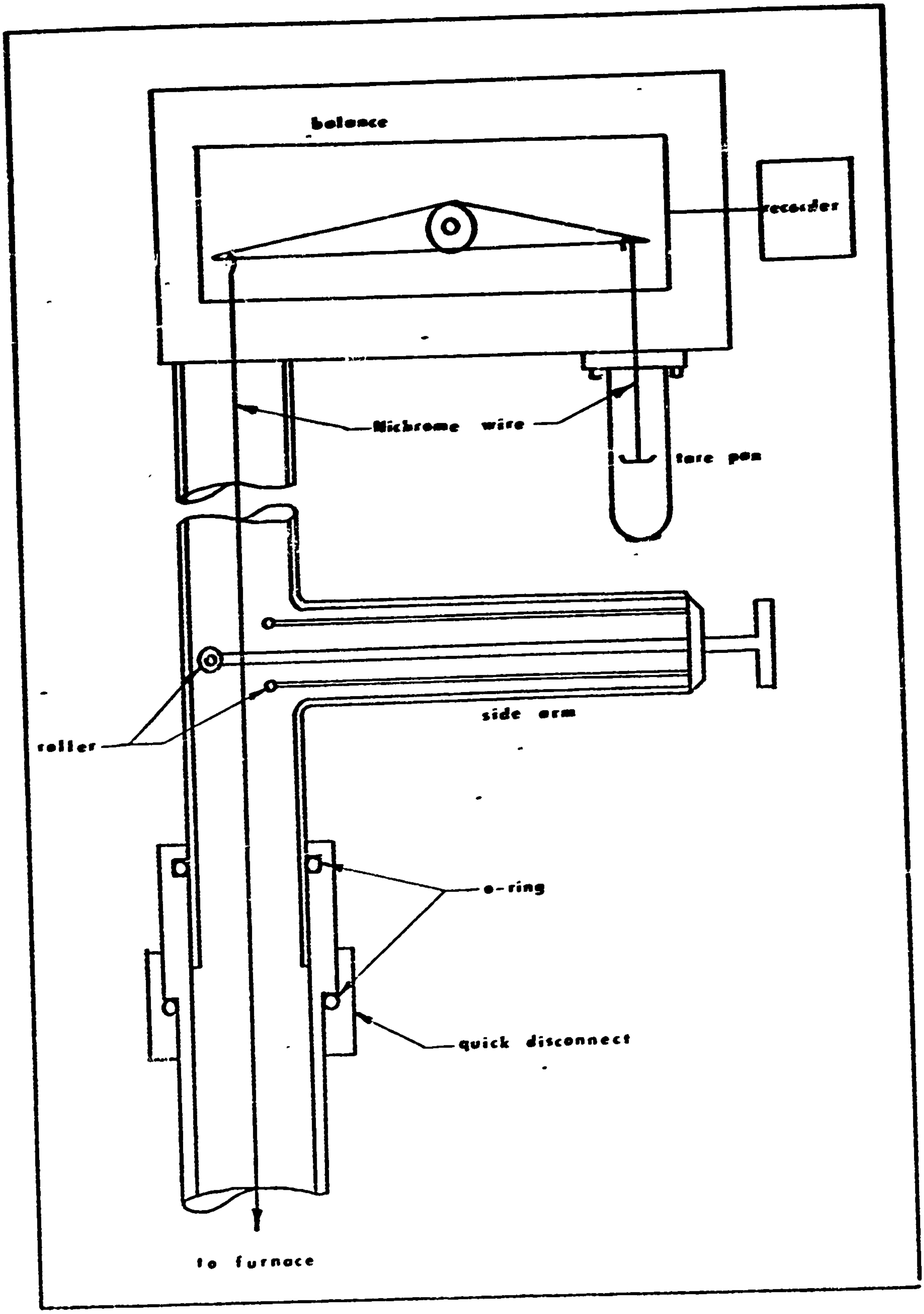

Fig. 8. Balance and Suspension System Arrangement

exceeding the scale of the recorder, but within the limits of the balance, could be adjusted so the recorder trace was always within the recorder range. The amount of biasing necessary was indicated on the potentiometer and thus the weight change was always known. Capacity of the balance was 100 grams and weight changes on the order of 10 micrograms could be measured. The balance was rigidly mounted in a vacuum chamber which housed the same gas environment as the sample area.

Suspended from one side of the balance by a Nichrome wire was a tare pan for holding weights to bring the balance output within the range of the recorder. Suspended from the other side of the balance, also by a Nichrome wire, was a platinum counterweight and a platinum hook for suspending samples. At approximately the midpoint of the counterweight wire was located a side arm for raising and lowering the counterweight and any sample suspended from it.

The sample suspension techniques for the two types of weight measurements made in this study are shown in Fig. 9. The samples and suspension are shown in the proper position for making a run. The shield assemblies have not been shown for clarity. The technique for vaporization measurements involved hanging an alumina crucible by a platinum hook from the Nichrome balance wire. The crucible was heavy enough to act as a counterweight and thus the platinum counterweight was not needed for vaporization runs. The samples for the vaporization runs were introduced from the bottom of the furnace by means of the previously mentioned insertion assembly. The inset shows how the sapphire hook was held by the alumina rod to prevent turning of the sample. The sapphire hooks for both types of runs were formed with a torch from 0.02 inch diameter sapphire rods. Weight change runs involved hanging the sample with sapphire hooks directly from the platinum counterweight as shown.

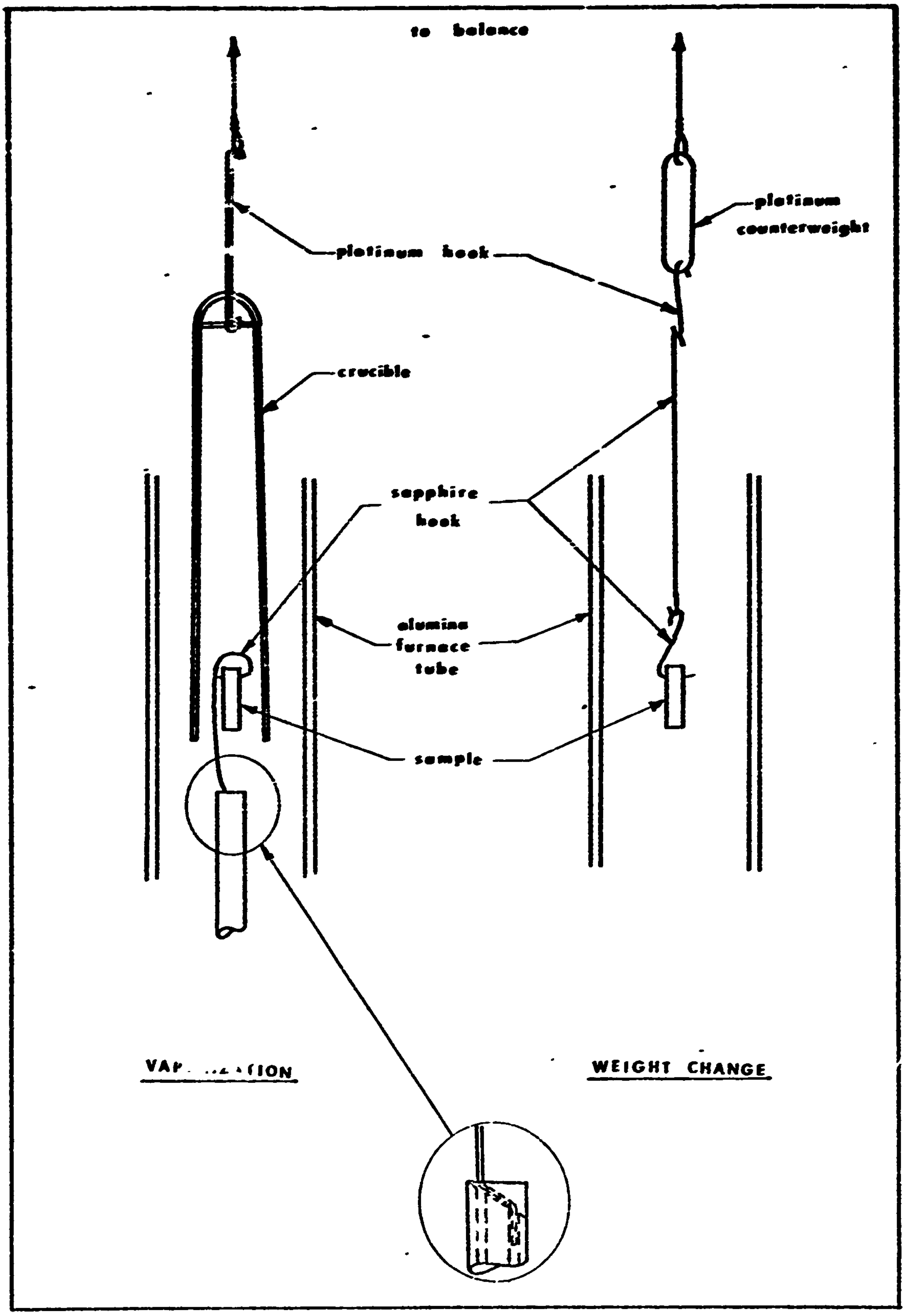

Fig. 9. Sample Suspension Techniques

IV. Experimental Procedure

Sample Preparation

As previously mentioned the samples were received from Norton Company in the form of 1/8 inch square bars. Prior to any sample preparation, bars known to come from different billets were X-rayed to obtain a standard X-ray pattern for each billet and its associated bars. The X-ray procedure will be discussed in a later section of this chapter.

The bars were then mounted on glass plates with mounting wax, and cut with a diamond saw into smaller bars approximately 1/2 inch long. Still mounted on the glass plates, each of the smaller bars had a 0.030 inch hole drilled through the bar near one end for suspending the bars on the sapphire hooks. The drilling was done with a Sheffield Cavitron Ultrasonic Machine Tool. After drilling, the samples were removed from the glass and cleaned of all traces of the mounting wax, using an ultrasonic cleaner.

For each high temperature run a sample was first measured with a centimeter micrometer to find the average length of each of the three dimensions. Several measurements were made in each dimension to arrive at the average. Using the three averages the surface area of the sample was computed. No allowance was made for the hole because the area of the hole was small compared to the total area of the sample.

After the sample was measured, it was cleaned with acetone and then with alcohol. The sapphire hooks to be used during the thermogravimetric measurement were also cleaned at this time with acetone and alcohol. During and after cleaning, the sample and the hooks were carefully handled with clean forceps to prevent contamination by such things as natural skin oil. The sample and the hooks were then weighed separately several times to obtain an average weight for each. A Mettler H20 balance was used to determine the weights to the nearest 10 micrograms. The sample and the hooks were now ready to be placed in the furnace.

Weight Change Measurement

Prior to placing the sample and the hooks into the furnace the temperature in the sample area was adjusted to the predetermined temperature of the run. If the furnace was off, this was accomplished by manually increasing the power to the heating element over a period of 3 to 4 hours until the desired temperature was reached. By slowly increasing the furnace temperature, two possible damaging things were avoided. First, hot spots in the furnace were avoided, and second, outgassing of furnace components was slow enough to prevent oxidation of the tungsten heating element.

If, however, the furnace had been at a temperature above 1000°C for several days the temperature was manually adjusted more rapidly to the desired temperature using as a guide an upper limit pressure of 1×10^{-4} on the furnace ionization gauge. In either case once the desired temperature had been attained manually, the furnace control was switched to the automatic mode and the digital set point circuit was adjusted to hold the temperature.

The next step was to carefully place the correct tare weight on the balance tare pan. For the first run this was largely experimental, but for succeeding runs a correction factor obtained from the first run was merely added to the combined weights of the sample and the hooks to arrive at the required tare weight. Once the tare weight was in place the sample and the hooks were suspended from the other side of the balance. However, the sample and the small hook it was suspended from were not hung in the position shown previously in Fig. 9. Instead they were suspended directly from the counterweight. In this position, the sample could be lowered with the side arm, but it would never reach the hot portion of the sample area.

The system was then sealed and pumped down to a pressure of 500 microns. Oxygen was then admitted until the pressure in the system reached 150 torr. Running conditions were then established in the sample area. If static conditions were desired, the sample area was closed off from all system components except the balance and the Wallace-Tiernan gauge. If flowing conditions were desired, the two needle valves were adjusted to maintain a total pressure of 150 torr and a flow rate of approximately 70 cubic centimeters of gas per minute.

After running conditions were established the arrested sample and hooks were lowered by means of the side arm into the furnace. The recorder was then turned on to the two milligram full scale setting and the potentiometer adjusted to bring the recorder trace within scale. The recorder trace was allowed to stabilize (approximately 15 minutes) to obtain a "zero weight" for the sample.

Without touching the potentiometer, the recorder was turned off and the sample was arrested with the side arm. Using oxygen, the system was then pressurized to ambient pressure, being careful to not disturb the settings of the two needle valves if flowing conditions were required. A slight change in the flow rate shifted appreciably the trace on the recorder. Pressure changes also shifted the recorder trace, but not near as much as flow rate changes.

The system was then opened and the sample was suspended in the running position shown in Fig. 9. However, the sample was still arrested by the side arm and not yet in the hot sample area. The system was again sealed and pumped out. This time, though, it was pumped out to 150 microns and then pressurized to 150 torr again with oxygen. If static conditions were required, they were established as before; but if flowing conditions were required, the flow was established without disturbing either needle valve. At this point the flow, if desired, was diverted through the carbon dioxide trap and/or the saturator. This did not affect the flow nor shift the recorder trace.

After allowing approximately 15 minutes for stabilization of the system (less if static) the temperature was checked and adjusted if necessary. The sample was then lowered into the hot sample area and the recorder was immediately turned on. The recorder was set on fast speed for the first 15 minutes and then shifted to slow speed for the remainder of the run.

If the carbon dioxide trap was being used, it was necessary periodically during the run to collect the carbon dioxide. The first step of the collection procedure was to temporarily establish static conditions in the sample area without disturbing the needle valves. The cold trap was then sealed off and an evacuated balloon was attached to one valve. This valve was then opened and the cold trap was removed from the liquid nitrogen. The previously mentioned ascarite bulb system was then connected to the other valve of the cold trap. When the balloon indicated a positive pressure in the cold trap the valve to the ascarite bulbs was opened. The gas in the balloon was then forced back into the cold trap and the balloon valve was closed. Oxygen was then connected to the balloon valve to sweep the cold trap of all the carbon dioxide it contained. The cold trap was then replaced in the system and flow conditions were reestablished. The weighed ascarite bulb was then reweighed to determine the amount of carbon dioxide collected.

After a planned number of hours (usually 48) the recorder was turned off and the sample arrested. Again using oxygen the system was pressurized to ambient pressure and opened. Using forceps, the sample and hooks were retrieved and then weighed on the Mettler balance.

Vaporization Measurement

The procedure for vaporization measurements is very similar to that used for weight change measurements. Therefore, only the differences between the two will be pointed out in this section.

First, because much of the crucible in a vaporization run was out of the hot zone and because of the size of the crucible, a recorder trace using flowing oxygen was very erratic. Hence vaporization runs were made only in static environments.

Second, the crucible was hung from the balance and the sample was set in the insertion assembly as shown in Fig. 9. Static conditions were then set up as before with the sample pulled down out of the hot zone. Then with the crucible in the hot zone the recorder was turned on.

Third, once a stable trace was attained with the crucible, the sample was raised into the position under the crucible shown in Fig. 9.

Fourth, after the planned number of hours, the sample was pulled down from the hot zone, but the crucible was kept at the static conditions of the run for approximately 6 hours. This 6-hour period was needed to determine how much of the weight gain on the crucible was attributable to deposition of platinum vaporizing from the thermocouples.

X-Ray Analysis

As previously mentioned, a sample from each billet was X-rayed to obtain a standard X-ray pattern. After the oxidation and second weighing of a sample, the sample was X-rayed on several sides. The X-ray unit used was a North American Philips Company, Inc. type 2045B/3 machine with a copper X-ray tube. Standard X-ray diffraction techniques were used and care was taken to be sure that each X-ray pattern was obtained under the same conditions as the standard pattern.

The X-ray patterns obtained from the oxidized samples were then compared with the standard pattern. Comparing the patterns readily showed where new peaks existed in the "oxidized" pattern. Then using known patterns of suspected oxide products, the constituent attributable to each new peak was determined.

High temperature X-ray work was done on a General Electric XRD5 X-Ray spectrogoniometer. As with the low temperature X-ray work, copper K_α radiation was used. The silicon carbide was first prepared by grinding and then sifting through a 325 mesh sieve. The powder was then applied to a platinum heater in an acetone slurry. To the back side of the heater was attached a thermocouple for monitoring the temperature. The heater and the thermocouple were then placed in the sample chamber of the X-ray machine. The heater was connected to a power source and the thermocouple to a potentiometer. An X-ray pattern was then obtained for the powdered silicon carbide. The heater was then turned on and power was applied until the desired temperature was reached. X-ray patterns were then obtained for the oxidizing sample while it was at temperature. As with the low temperature patterns, comparisons were made to determine the oxidation products.

Metallograph Analysis

After X-raying, the next step was to cross-section, mount, and polish a sample in preparation for analysis under the metallograph. The samples were cut with a diamond saw and then mounted in Bakelite. Pieces of brass were also mounted in the Bakelite with the sample. The brass helped control rounding of the mount during polishing. Samples were polished first through 600-grit carborundum paper. The samples were then polished on a wheel with 3 micron and 1/4 micron diamond pastes. The diamond paste was removed by flushing with alcohol and the alcohol was evaporated with a heat gun.

A Bausch and Lomb Research II Metallograph was then used to obtain high magnification Polaroid prints of each cross-sectioned sample. The area of prime interest on each sample was the oxide-matrix interface. Photographs were taken of areas of the interface which were representative of the entire sample.

Probe Analysis

To determine what elements were in the matrix and oxide layer of the cross sections observed under the metallograph, an electron probe was utilized. The probe made by Applied Research Laboratories was capable of detecting the presence of different predetermined elements in a sample. However there were some limitations to the machine. The important limitations were that only elements in sufficient quantities (depends on the element, what form it is in, and its distribution in sample) were detected, and only the presence and not the quantity of the element was detected. Output from the probe was directed to an oscilloscope. Polaroid prints were made with an attachment that used the oscilloscope trace as the light source. Light spots on the prints indicated a presence of the element in question, and dark areas indicated the absence of the element.

V. Results and Discussion

Table III is a summary of the samples oxidized and the conditions under which the oxidation took place. The samples containing the tungsten and the cobalt are marked with an asterisk. As previously mentioned, the tungsten was in the form of tungsten carbide. Because of this and the presence of cobalt, it was believed that the silicon carbide was ground with a tungsten carbide wheel with cobalt as the binder. This belief, however, was not confirmed by Norton Company since the silicon carbide was still being researched and the information was therefore proprietary.

TABLE III

Summary of Oxidation Runs

Sample Number	Temperature	Condition[§]	Oxygen	Run Duration
1	1300°C	static	as-received	48 hrs
2	1400°C	static	as-received	48 hrs
3	1400°C	flowing	as-received	48 hrs
4	1500°C	static	as-received	48 hrs
5	1500°C	flowing	cleaned	48 hrs
6[†]	1500°C	static	cleaned	54 hrs
7	1600°C	static	as-received	48 hrs
8*	1400°C	flowing	cleaned	48 hrs
9*	1500°C	flowing	cleaned	48 hrs

---

*Contains small amounts of tungsten carbide and cobalt, as per Table II.

[†] Vaporization measurement.

[§] All samples were run at a total oxygen pressure of 150 torr.

Thermogravimetric Data

Figures 10, 11, 12, and 13 show the thermogravimetric results in the form of weight change per unit area in milligrams per square centimeter versus time in hours. The numbers in parentheses indicate the sample number in Table III. As shown in Fig. 10, a big jump in the rate of oxidation was observed from 1400°C to 1500°C. To determine the reason for the jump, an oxidation run at 1500°C using cleaned oxygen was made. The results for the two 1500°C runs are shown in Fig. 11. The reason for the jump was due to the water vapor in the as-received oxygen. This is in agreement with Jorgensen (Ref 20), Lea (Ref 28) and Suzuki (Ref 16). Enough samples were not available to determine the magnitude of the same expected jump at the other temperatures. However, the available results do indicate that because of water vapor, 1400°C can be considered the practical upper temperature limit under similar oxidation conditions for the silicon carbide tested.

Figure 12 shows the data for the oxidation of the silicon carbide samples marked with an asterisk in Table III. It should be noted that the scale of the ordinate is changed and that comparing this data with the previous data shows the new material to have slower rates of oxidation. Although the primary difference between the two sample types is tungsten carbide and cobalt, Table II also shows other differences. Therefore, it could not be determined what elements or compounds were contributing to the slower rates observed. Time did not permit oxidation runs using oxygen with water vapor, but increased rates were expected based on the similarities between the oxide layers of these samples and the layers of previous ones. These similarities will be pointed out later in this chapter.

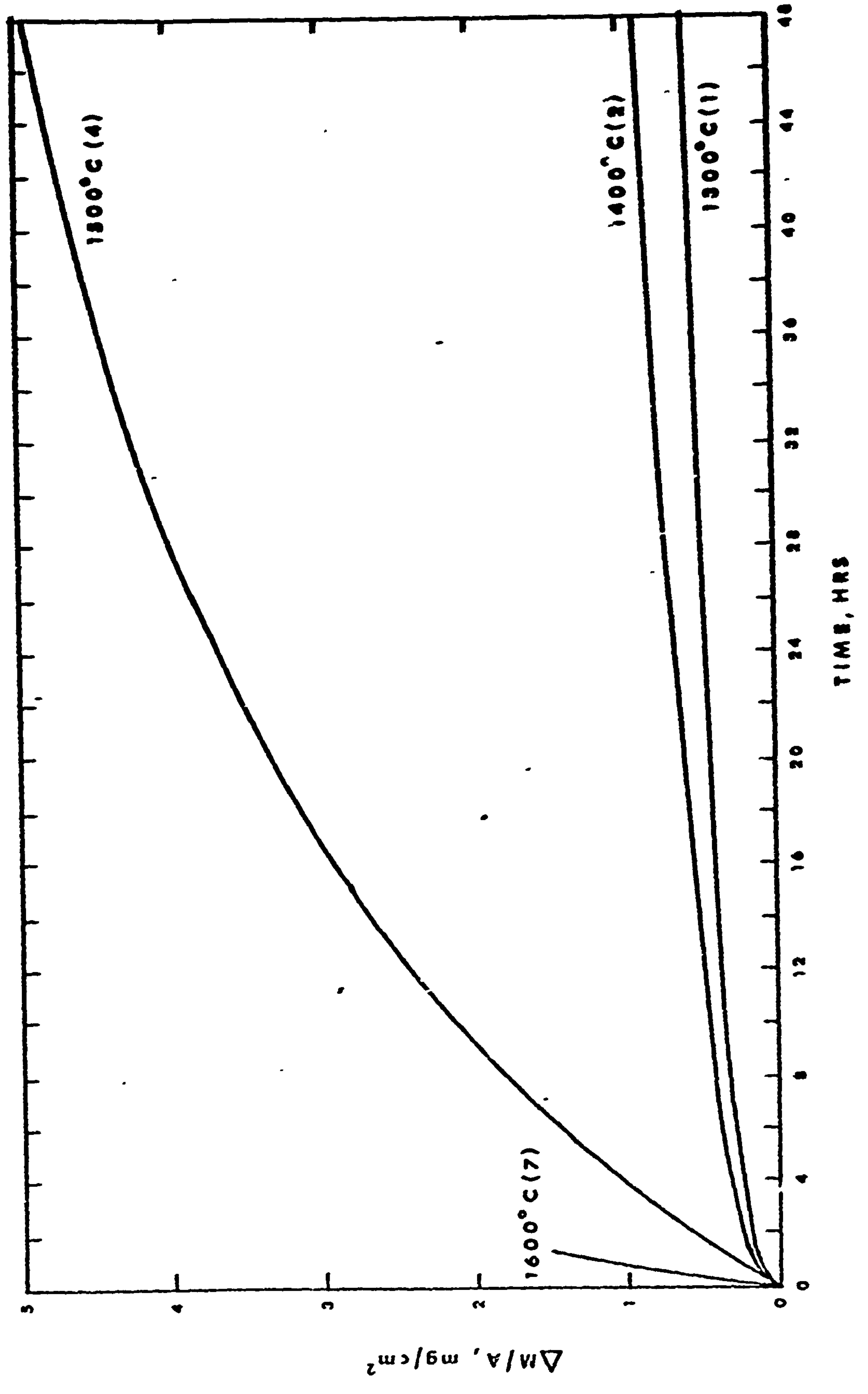

Fig. 10. Weight Gain per Unit Area vs Time for SiC in As-Received Oxygen at a Total Pressure of 150 Torr under Static Conditions

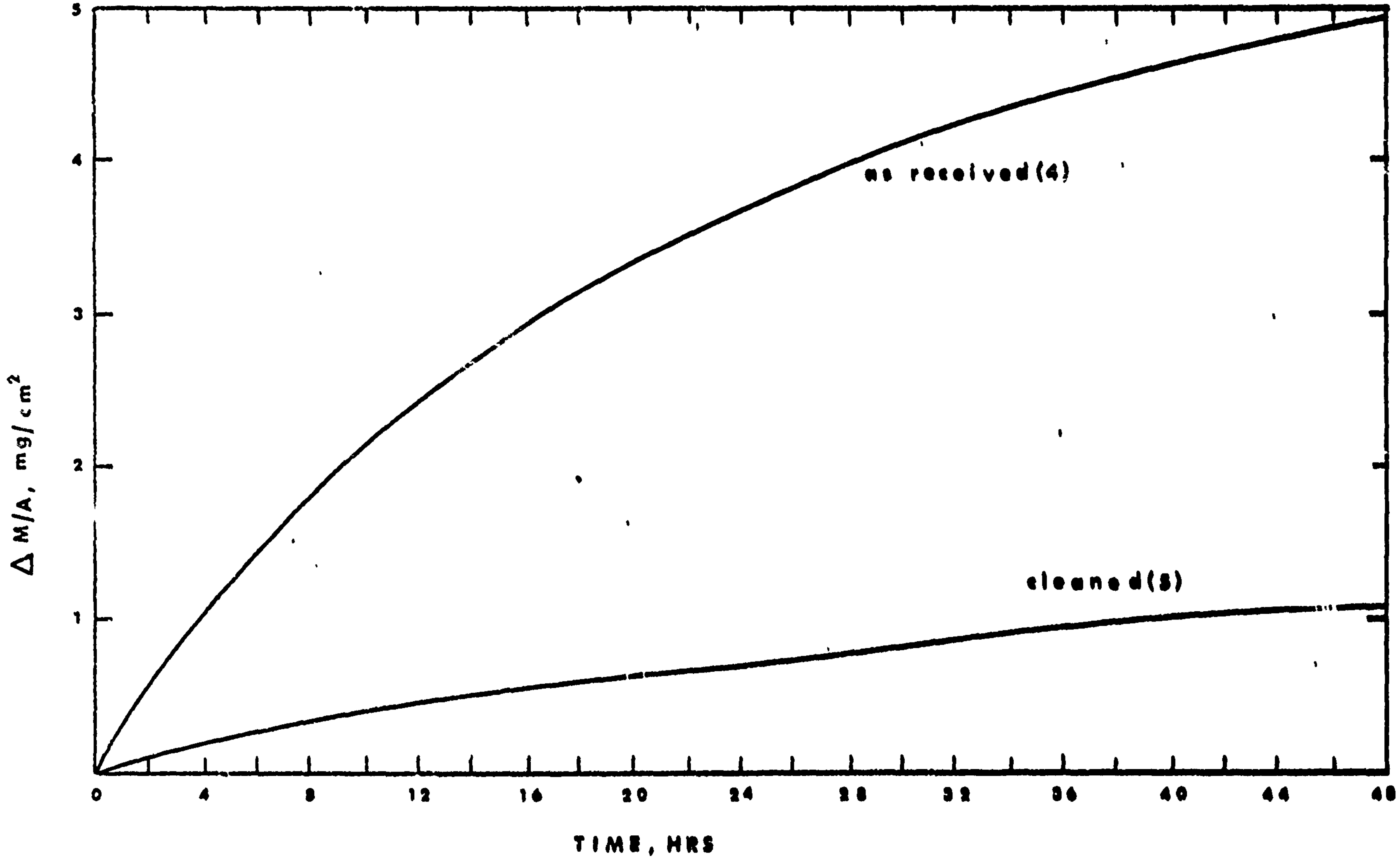

Fig. 11. Weight Gain per Unit Area vs Time for SiC at 1500°C in Oxygen at a Total Pressure of 150 Torr

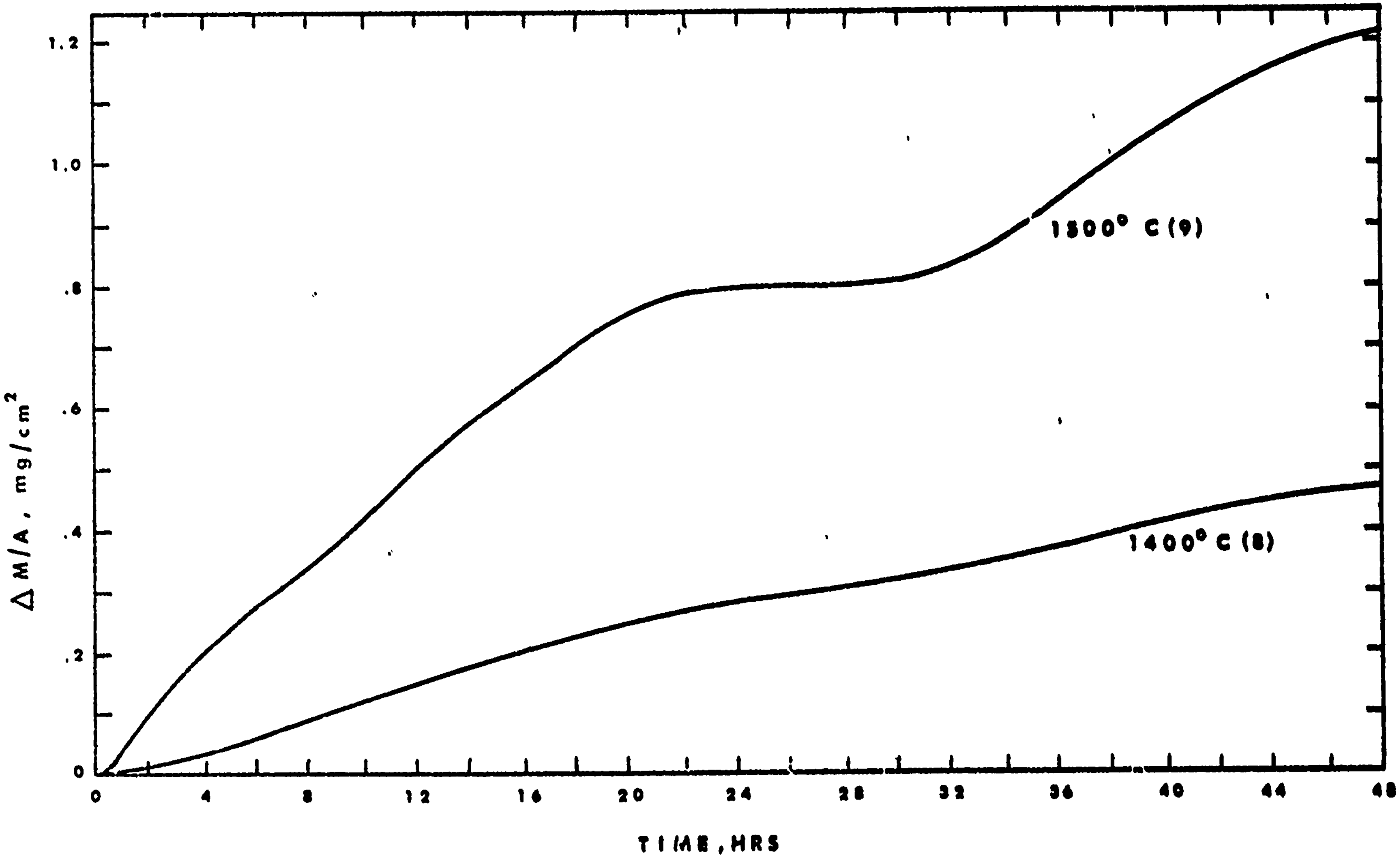

Fig. 12. Weight Gain per Unit Area vs Time for SiC (with WC and Co) in Cleaned Oxygen at a Total Pressure of 150 Torr under Flowing Conditions

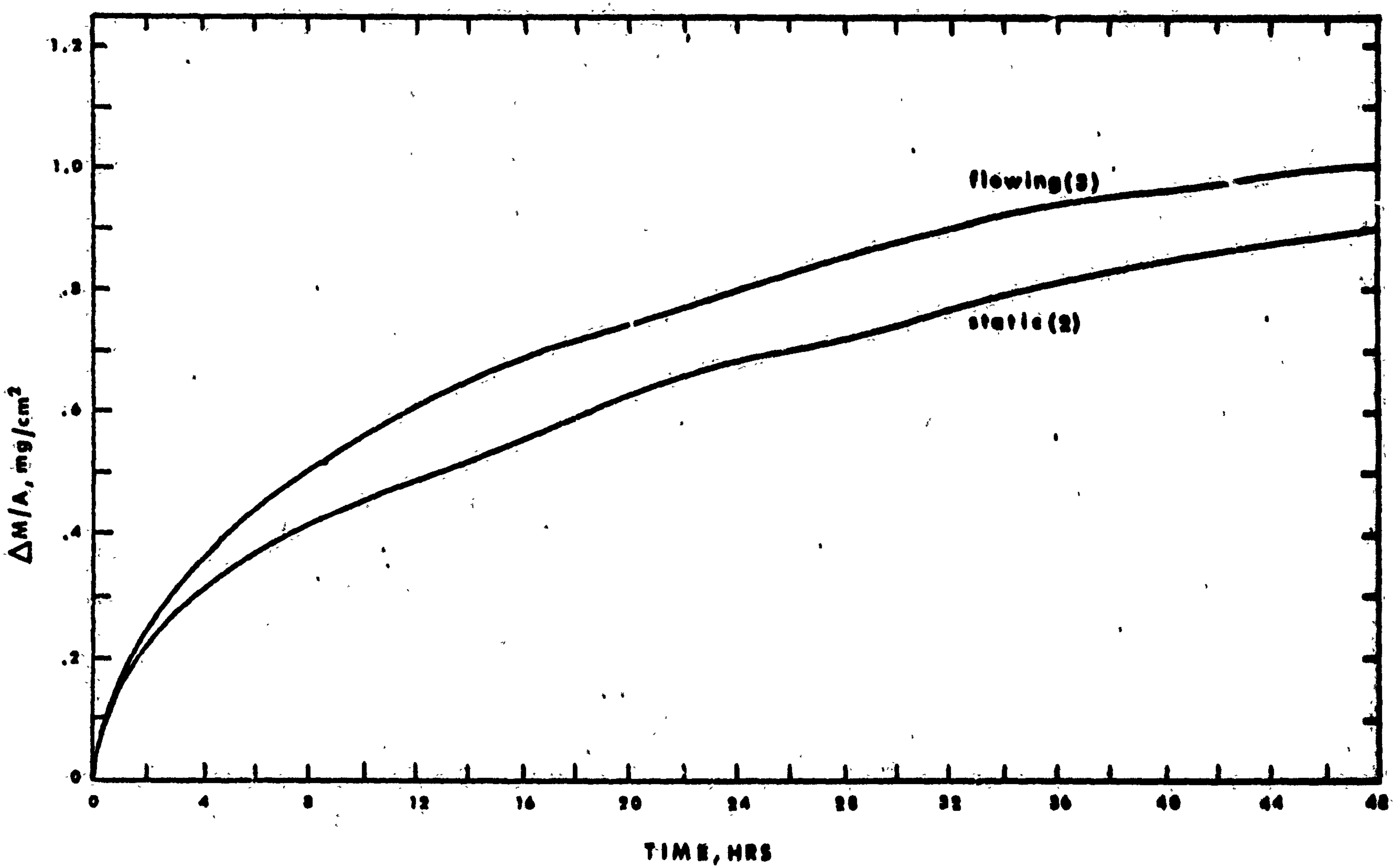

Fig. 13. Weight Gain per Unit Area vs Time for SiC at 1400°C in As-Received Oxygen at a Total Pressure of 150 Torr

Figure 13 shows a comparison between flowing and static conditions at 1400°C. The difference is approximately 10% and is well within experimental accuracy. Over long periods of time, balances of the type used in this study have been known to drift amounts greater than the difference shown.

Upon careful examination of the graphs for weight gain versus time, some undulation was noted in the traces, although it is not very obvious in the case of samples number 4 and 7. These changes in oxidation rates were caused by ruptures in the oxide layer exposing unoxidized matrix material. Rapid oxidation took place and the rate increased until the rupture had been "healed" with a new oxide layer. Further evidence of this will be given later in this chapter.

Sample number 6 was a vaporization measurement. Compared to the weight gain of the sample, the weight gain of the crucible due to condensible vapors was virtually nonexistant. This indicated that at temperatures at or below 1500°C and at oxygen pressures above 150 torr, the only appreciable vapor species leaving the oxidizing silicon carbide were either carbon monoxide, carbon dioxide or both. The fact that one or both of the oxides of carbon was leaving the surface was verified by using the carbon dioxide trap. Unfortunately, qualitative results were not obtained, but a color change of the ascarite from brown to white during collection indicated that a carbon oxide had vaporized from the silicon carbide. Qualitative results were not found for the collection of carbon dioxide because contamination of the ascarite by water vapor could not be prevented.

Metallograph Data

Figures 14 and 15 show metallograph pictures of cross sections of

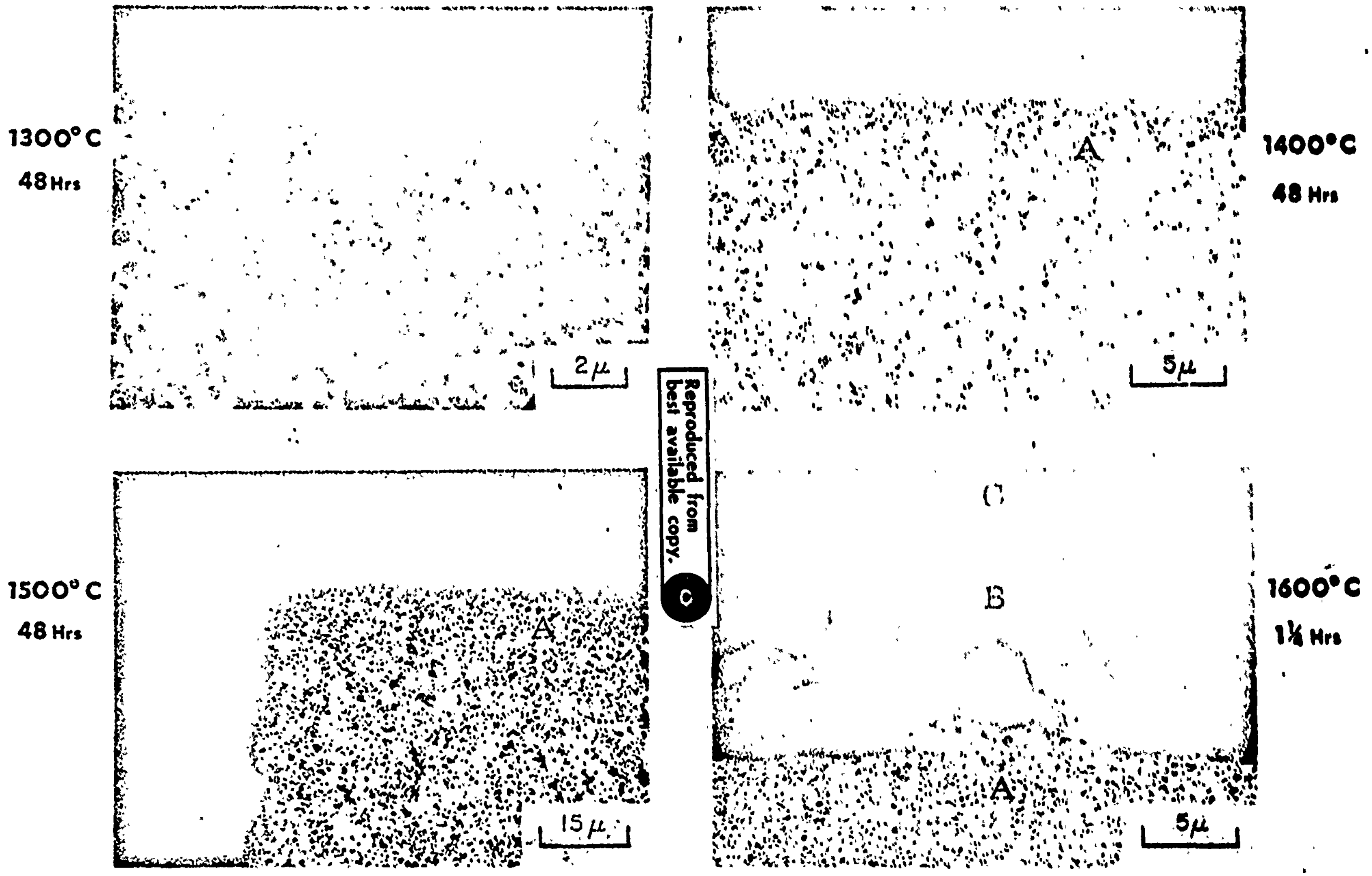

Fig. 14. Cross Sections of SiC Oxidized in As-Received Oxygen

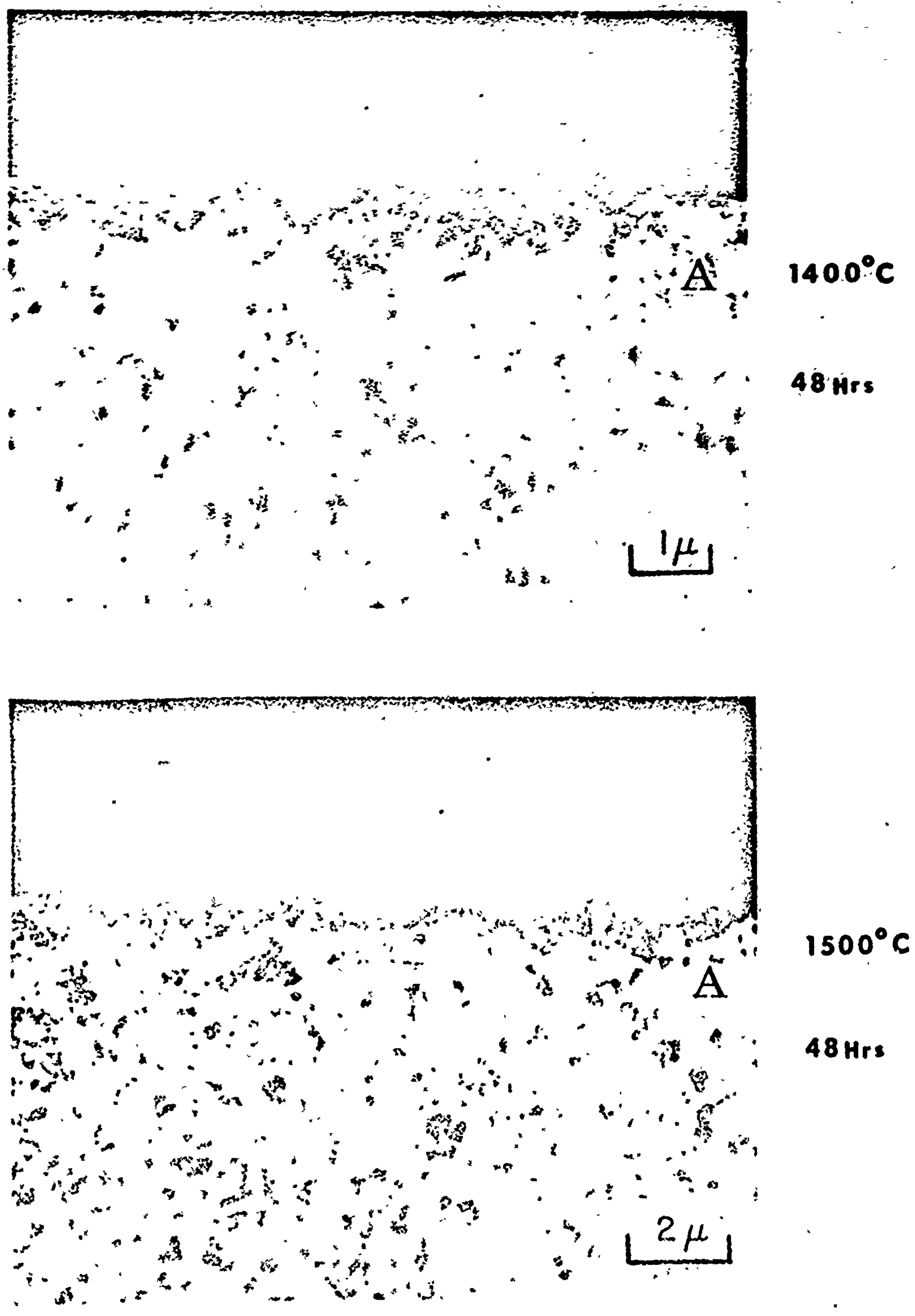

Fig. 15. Cross Sections of SiC Oxidized in Cleaned Oxygen

the silicon carbide samples. Figure 14 shows representative areas of samples oxidized in the as-received oxygen and Fig. 15 shows areas representative of samples oxidized in clean oxygen. The light area (A) in each photograph is the silicon carbide matrix. The gray band (B) immediately adjacent to the matrix is the oxide layer. The remaining dark area (C) is the epoxy or Bakelite used to mount the samples.

In Fig. 14 the holes in the oxide were due to trapped carbon monoxide or carbon dioxide. These holes are a clear indication that the oxide was an amorphous phase. The holes also indicate that the diffusing species during oxidation was oxygen diffusing through the oxide layer to the silicon carbide in agreement with Jorgensen (Ref 6), and that the reaction took place at the silicon carbide--oxide interface. If silicon carbide had been the diffusing species there would not have been bubbles in the oxide.

It was observed, except in the sample oxidized at 1600°C, that the oxide layers were continuous and fairly uniform over the entire surface of the samples. Physical evidence of rupture was also observed in these samples; this phenomenon was believed to be the reason for the undulating weight gain traces.

The sample oxidized at 1600°C did not have a uniform oxide layer over the sample. Instead, the surface was covered with large oxide beads spaced approximately one millimeter apart with a very thin oxide film between beads. A cross section of one of the beads is shown in the 1600°C photograph. It was believed that the bead formed in the following manner: As the oxide rapidly grew on the surface of the sample some carbon monoxide or carbon dioxide was trapped under the oxide layer. As more gas formed, the carbon oxide bubble expanded to reach a state of lower energy.

The expanding bubble pushed the vitreous oxide layer in front of it, thus causing the oxide from the surrounding areas to flow towards the bubble. Physically, this is very similar to water beading up on a polished surface.

By comparing the oxide layers of the samples oxidized with as-received oxygen with the layers of the samples oxidized with cleaned oxygen, it was observed that the cleaned oxygen resulted in thinner layers and fewer bubbles. There was, however, evidence of rupture in the samples oxidized in the cleaned oxygen. This was expected since the energy to break through a thin layer is less than that required to break through a thick layer.

X-Ray Data

In all samples, physical observations and X-ray traces showed the presence of an amorphous oxide layer. However, the X-ray traces also showed the presence of crystalline phases in the oxide. One crystalline phase which appeared in all samples was alumina. Tridymite and α-cristobalite, two crystalline phases of silica, also appeared, and in one case (sample number 4) an aluminum silicate, mullite, was found. Mullite probably formed in other cases too, but there was not a sufficient amount for the X-ray traces to show it. Sample number 4 gained the most weight and therefore had the most alumina in the oxide layer. Assuming that the alumina was uniformly spread through the sample, then as oxidation took place the matrix surface receded exposing the alumina. Although the percentage of alumina to silica in the oxide was probably the same for each sample, the more of each there was the greater was the possibility that any chemical combination of the two would be seen in the X-ray traces.

Although it could not be confirmed (again proprietary information), aluminum was believed to be uniformly spread through the matrix in the form of alumina. Alumina is sometimes used as a grain growth inhibitor.

Since there was no evidence of any other grain growth inhibitors in the sample it was assumed that alumina was being used for that purpose.

Tridymite and α-cristobalite did not appear together except in two cases, samples 8 and 9. Except for 8 and 9, tridymite was observed in only X-ray traces of samples that were run under static conditions, and α-cristobalite was observed in only X-ray traces of samples run under flowing conditions. In the case of samples numbers 8 and 9, the X-ray trace of the material before oxidation indicated the presence of some tridymite. The tridymite was removed before oxidation with hot hydrofluoric acid. Because conditions were flowing during oxidation, it was then expected that α-cristobalite would be the crystalline phase appearing. A possible explanation for the appearance of both is that the flowing gas nucleated α-cristobalite and tridymite particles not removed with the acid nucleated more tridymite.

It should be noted that the primary silica phase in all samples was the amorphous phase. The amorphous nature of the oxide was also more predominant when cleaned oxygen was used. These results were expected and are in agreement with Wagstaff (Ref 12) who found devitrification enhanced with the presence of water vapor.

In an effort to determine whether the crystalline phases of silica were present during oxidation or whether they appeared on cooling, high temperature X-ray traces were obtained. The traces showed that in air the crystalline phase, α-cristobalite, was present at both 1400°C and 1500°C.

Probe Data

Figures 16, 17, and 18 are photographs of probe scans for different chemical elements on three different samples. Figure 16 is representative

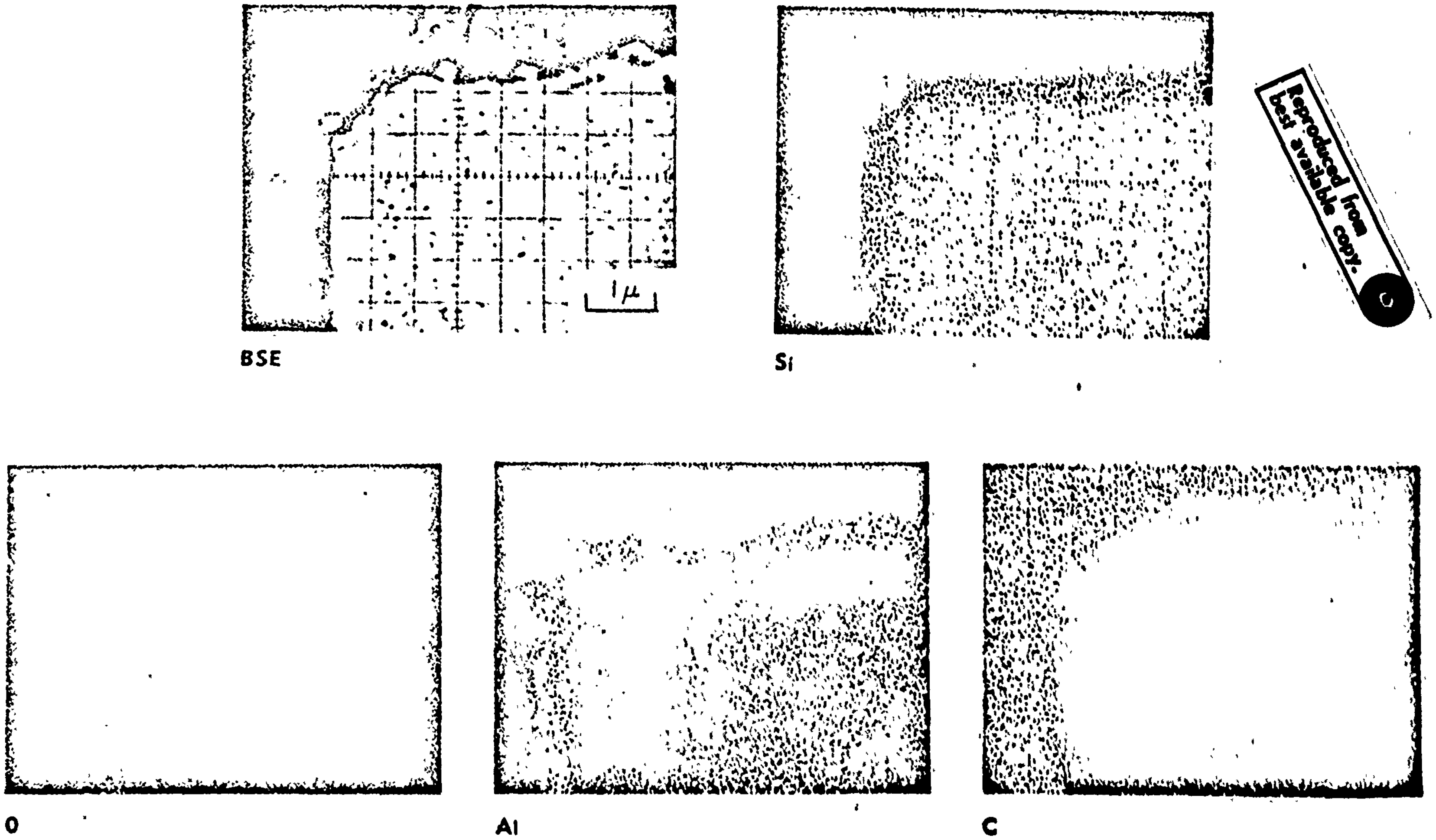

Fig. 16. Probe Scan of Cross Section of SiC Oxidized in As-Received Oxygen

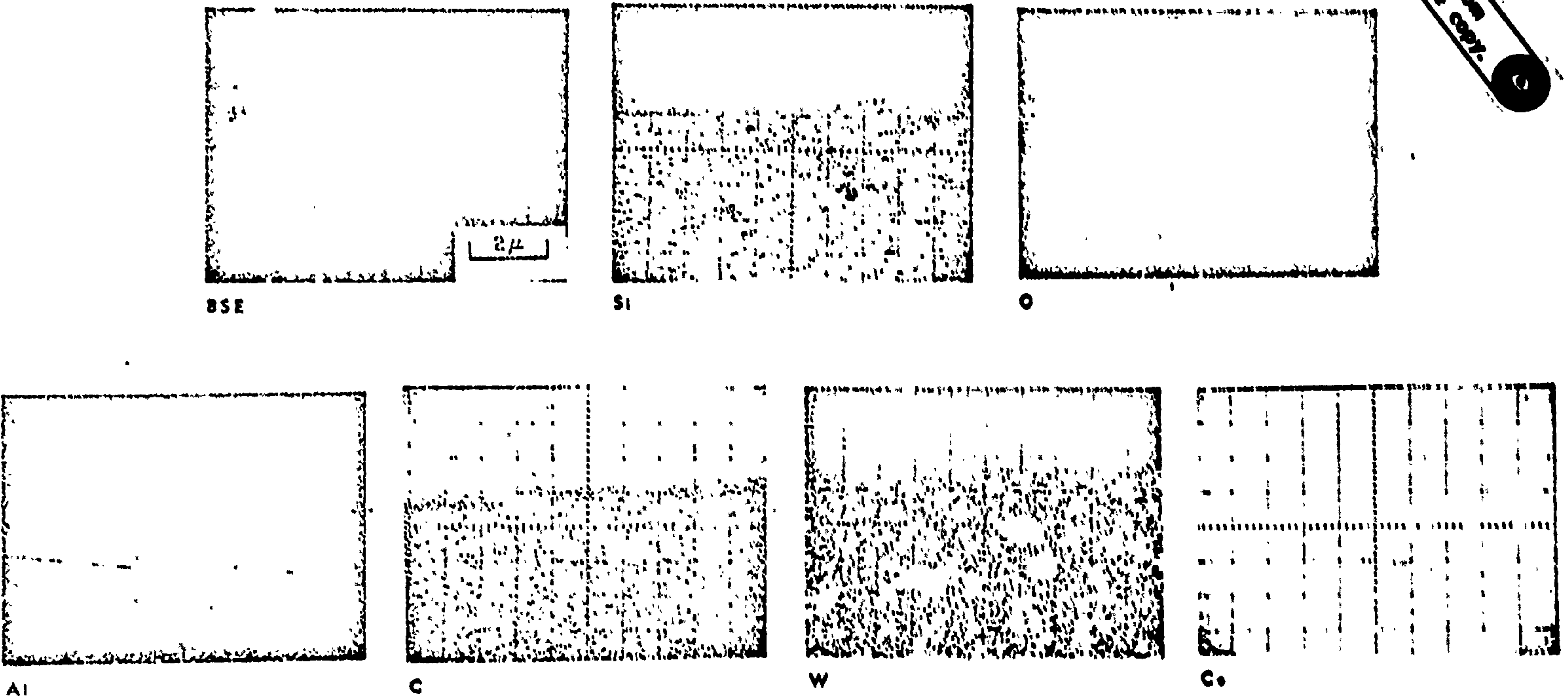

Fig. 17. Probe Scan of Cross Section of SiC (with WC and Co) Oxidized in Cleaned Oxygen

Fig. 18. Probe Scan of Cross Section of SiC Oxidized in As-Received Oxygen at 1600°C

of all the oxidized samples except 7, 8, and 9. Figure 17 is representative of samples 3 and 9, and Fig. 18 shows the bead on the 1600°C sample (number 7). Probe scans were made for a wide variety of elements, but only those elements that were positively identified with a sample are shown with that sample. Other elements were present in the samples as shown by the mass spectrographic analysis, but the quantities were too small to be detected with the probe. The scan for a particular element is indicated by its chemical symbol. BSE stands for back scatter electron and is a picture, similar to a metallograph picture, showing the area probed. In all cases the large light area in the BSE picture is the matrix and the gray band is the oxide layer. The dark area is again either the Bakelite or epoxy mount.

To eliminate some confusion it should be pointed out that the probe could not distinguish between the sample and the mount. Therefore, with the epoxy mount used for the sample shown in Fig. 18 it was expected that the probe would show a presence of silicon, carbon, and oxygen in the mount as well as the sample. With the samples shown in the other two figures, Bakelite mounts were used. Therefore, scanning across these mounts showed traces of carbon and oxygen.

Figure 16 shows that there was silicon, aluminum and oxygen spread uniformly through the oxide layer. Also the concentration of aluminum was greater in the oxide than in the matrix. This supports the belief that as the silicon carbide surface recedes, the exposed alumina congregated in the oxide layer.

The probe trace for oxygen shows an abundance of oxygen in the oxide layer as well as oxygen in the matrix. This further supports the belief that the aluminum in the samples was in the form of alumina.

The probe trace for carbon shows clearly that there was no carbon in the oxide. What carbon may appear to be there is either carbon trapped as a carbon oxide bubble under the surface or diamond past that remained from polishing.

The trace for silicon shows that there was a greater abundance of silicon in the matrix than in the oxide. This was expected since the density of the matrix is higher than the density of the oxide.

Figure 17 shows not only the same things Fig. 16 did, but it also shows where the tungsten and cobalt were located in these samples. The trace for cobalt shows that the cobalt in the matrix was uniformly distributed. What appears to be cobalt in the oxide and the mount was only "noise" on the probe.

By comparing the BSE trace and the traces for tungsten and silicon it was readily apparent that the bright particles in the matrix on the BSE trace were tungsten carbide particles. These bright spots also matched up with the areas void of silicon on the silicon trace.

Figure 18 shows the same bead seen earlier in Fig. 14. Figure 14 showed quite clearly two different bands of material within the bead. This is not shown clearly on the BSE photograph, but the probe traces for silicon, aluminum, and oxygen clearly indicate the reason for the bands seen earlier. The traces indicate that the inner band was alumina and the outer band was silica. It was believed that the formation of the bands was a physical phenomena and not a chemical phenomena. The phenomena was possibly a cooling effect or possibly an effect due to the beading up of the oxide.

VI. Conclusions and Recommendations

Based on the results of this study, the following can be concluded:

1. From an oxidation standpoint the silicon carbide studied can be used up to and including a temperature of 1400°C in environments containing approximately 150 torr of oxygen. Above this temperature water vapor causes a marked increase in the rate of oxidation.
2. The oxidation reaction can be represented by the equation

$$SiC + \left(1+\frac{x}{2}\right)O_2 \longrightarrow SiO_2 + CO_x \qquad (14)$$

   where the carbon oxide may be carbon monoxide or carbon dioxide. The equation is valid because vaporization of condensible vapors was shown to be negligible and the alumina was shown to be inactive in the oxidation reaction.
3. The product of the oxidation reaction is a protective layer of silica containing primarily amorphous silica. The crystalline phases tridymite and α-cristobalite may also be present, particularly if water vapor is present.

Some recommendations need to be made concerning further study of the oxidation of hot pressed silicon carbide and precautions that might be taken to avoid difficulties. These are as follows:

1. Because samples in this study varied, enough samples of one type should be obtained to effectively investigate future work.
2. A different method should be devised for recovering the solid carbon dioxide from the cold trap.
3. With silicon carbide powders, oxidation rates are known to be dependent on oxygen pressure. This dependence should be investigated

for the hot pressed silicon carbide.

4. The effect of water vapor on the oxidation rate should be investigated further.
5. The mechanism of alumina segregation should be investigated.

Bibliography

1. Brodsky, M. B., and D. Cubicciotti. "The Oxidation of Silicon at High Temperatures." Journal of the American Chemical Society, 73: 3497-3499 (July 1951).

2. Law, J. T. "The High Temperature Oxidation of Silicon." Journal of Physical Chemistry, 61:1200-1205 (September 1957).

3. Evans, J. W. and S. K. Chatterji. "Kinetics of the Oxidation and Nitridation of Silicon at High Temperatures." Journal of Physical Chemistry, 62:1064-1067 (September 1958).

4. McAdam, D. J. and G. W. Geil. J. Research Natl. Bur. Standards, 28: 593 (1942).

5. Ligenza, J. K. and W. G. Spitzer. "The Mechanisms for Silicon Oxidation in Steam and Oxygen." J. Phys Chem Solids, 14:131-136 (1960).

6. Jorgensen, P. J. "Effect of an Electric Field on Silicon Oxidation." The Journal of Chemical Physics, 37:874-877 (August 1962).

7. Deal, B. E. and A. S. Grove. "General Relationship for the Thermal Oxidation of Silicon." Journal of Applied Physics, 36:3770-3778

8. Burkhardt, P. J. and L. V. Gregor. "Kinetics of the Thermal Oxidation of Silicon in Dry Oxygen." Transactions of the Metallurgical Society of AIME, 236:299-305 (March 1966).

9. Wagner, Carl. "Passivity During the Oxidation of Silicon at Elevated Temperatures." Journal of Applied Physics, 29:1295-1297 (September 1958).

10. Gulbransen, E. A. and S. A. Jonsson. "Thermochemical Analysis of the High Temperature Oxidation, Reduction, and Volatilization of Silicon and Silicon Carbide." Westinghouse Research Laboratories Report.

11. Brown, S. D. and S. S. Kestler. "Devitrification of High-SiO_2 Glasses of the System Al_2O_3 - SiO_2." Journal of the American Ceramic Society, 42:263-270 (June 1959).

12. Wagstaff, F. E. "Kinetics of Crystallization of Stoichiometric SiO_2 Glass in H_2O Atmospheres." Journal of the American Ceramic Society, 10:118-121 (March 1966).

13. Humphrey, G. L., Todd, S. S., Coughlin, J. P., and E. G. King. U.S. Bureau of Mines Report, 4888 (1952).

14. Keys, L. H. "The High Temperature Oxidation of Silicon Carbide." Thesis for the Degree of Doctor of Philosophy. University of New South Wales (1968).

15. Gulbransen, E. A., Andrew, K. F., and F. A. Brassant. "The Oxidation of Silicon Carbide at 1150°C to 1400°C and at 9×10^{-3} to 5×10^{-1} Torr Oxygen Pressure." Journal of the Electrochemical Society, 113: 1311-1314 (December 1966).

16. Suzuki, H. "A Study of the Oxidation of Pure Silicon Carbide Powders." Yogyoekyokai Shi, 65:88-93 (1957).

17. Adamsky, R. F. "Oxidation of Silicon Carbide in the Temperature Range 1200° to 1500°. Journal of Physical Chemistry, 44:258-261 (February 1961).

18. Jorgensen, P. J., Wadsworth, M.E., and I. B. Cutler. "Oxidation of Silicon Carbide." Journal of the American Ceramic Society, 42:613-616 (December 1959).

19. ----------. "Effects of Oxygen Partial Pressure on the Oxidation of Silicon Carbide." Journal of the American Ceramic Society, 43:209-212 (April 1960).

20. ----------. "Effects of Water Vapor on Oxidation of Silicon Carbide." Journal of the American Ceramic Society, 44:258-261 (June 1961).

21. Engell, H. J. and Hauffe. "Influence of Adsorption Phenomena on Oxidation of Metals at High Temperatures." Metallurgy, 6:285-291 (1952).

22. Antill, J. E., and J. B. Warbuton. "Oxidation of Silicon and Silicon Carbide in Gaseous Atmospheres at 1000-1300°C." Agard Conference Proceeding No. 52 (Pre-print) (October 1969).

23. Pultz, W. W., and W. Hertl. "$SiO_2 + SiC$ Reaction at Elevated Temperatures." Transactions of the Faraday Society, 62:2499-2504 (1966).

24. ----------. "$SiO_2 + SiC$ Reaction at Elevated Temperatures." Transactions of the Faraday Society, 62:3440-3445 (1966).

25. Abraytis, R. I., Mayauskas, I. S., et al. "Rate of Vaporization and Erosion of Silicon Carbide Based Ceramics." Materialy Dlya Kanala MGD-Generatoka (Material for the Channel of an MHD-Generator). 34-36 (1969).

26. Tripp, W. C. and R. W. Vest. "System for Measuring Microgram Weight Changes under Controlled Oxygen Partial Pressure to 1800°C." Vacuum Microbalance Techniques, 4:141-157 (May 1968).

27. Cahn, L. and H. R. Schultz. Vacuum Microbalance Techniques, 3:29 (1963).

28. Lea, S. C. "Oxidation of Silicon Carbide Refracting Materials." J. Soc. Glass Technol., 33:27-50T (1949).

Vita

Warren James Miller was born on 23 September 1948, the son of Leo Frederick Miller III and Elizabeth A. Miller. He lived with his parents in Waukesha, Wisconsin until 1965 when the family moved to Miami, Florida. He graduated in 1966 from Miami Palmetto Senior High School. He then attended the University of Miami in Coral Gables, Florida where he enrolled in the Air Force Reserve Officer Training Corps. Upon graduating with a Bachelor of Science degree in Mechanical Engineering he was commissioned a Second Lieutenant in the Air Force in June 1970. His initial assignment was to the Air Force Institute of Technology where he was enrolled in the Graduate Air Weapons Program.

Permanent address: c/o Mr. L. F. Miller
1380 Compamento
Miami, Florida 33156

This thesis was typed by Mrs. Virginia Blakelock.